Journal of Experimental Nanoscience
Publication details, including instructions for authors and subscription information:
http://www.informaworld.com/smpp/title~content=t716100757

Emergent methods to synthesize and characterize semiconductor CuO nanoparticles with various morphologies - an overview

Sambandam Anandan[a]; Shihe Yang[b]
[a] Nanomaterials and Solar Energy Conversion Lab, Department of Chemistry, Trichy 620 015, India [b] Department of Chemistry, Institute of Nano Science and Technology, Kowloon, Hong Kong

Online publication date: 01 December 2010

To cite this Article Anandan, Sambandam and Yang, Shihe(2007) 'Emergent methods to synthesize and characterize semiconductor CuO nanoparticles with various morphologies - an overview', Journal of Experimental Nanoscience, 2: 1, 23 — 56
To link to this Article: DOI: 10.1080/17458080601094421
URL: http://dx.doi.org/10.1080/17458080601094421

Journal of Experimental Nanoscience,
Vol. 2, Nos. 1–2, March–June 2007, 23–56

Taylor & Francis
Taylor & Francis Group

Emergent methods to synthesize and characterize semiconductor CuO nanoparticles with various morphologies – an overview

SAMBANDAM ANANDAN*† and SHIHE YANG‡

†Nanomaterials and Solar Energy Conversion Lab, Department of Chemistry, National Institute of Technology, Trichy 620 015, India
‡Department of Chemistry, Institute of Nano Science and Technology, The Hong Kong University of Science and Technology, Clear Water Bay, Kowloon, Hong Kong

(*Received 8 August 2006; in final form 30 October 2006*)

Nanotechnology can be defined as the science and engineering involved in the design, synthesis and application of materials and devices on the nanometer scale. It is not in itself a single emerging discipline, but rather a meeting of several traditional sciences such as chemistry, physics, materials science, biology and engineering to bring together the required expertise needed to develop these new technologies. The unique properties of nanoscale materials provide benefits in remediation, pollution prevention, and efficient use of resources; however, the greatest contribution to green chemistry is likely to be the new manufacturing strategies available through nanoscience. So, the present review mainly focuses on the synthesis of semiconductor CuO nanomaterials from different starting materials by adopting various routes such as vapor-solid, vapor-liquid-solid, solid-liquid, etc. to reveal the morphological features of the precursor.

Keywords: CuO; Nanomaterials; Nanorods; Nanotubes; Nanobelts; Nanowires; Synthesis; Alcohothermal; SEM; TEM; XRD

1. Introduction

Nanomaterials have attracted much attention in recent years because they are both important and interesting: important, as nanomaterials can have useful properties not exhibited by either small molecular systems or larger particulate matter; interesting, as working on supramolecular scales raises exciting synthetic challenges and allows intimate exploration of the relationships among atoms, molecules, and extended systems. Hence in recent years, synthesis and fabrication of one-dimensional (1D) nanostructured materials have received much research attention, due to their outstanding properties and potential applications of this class of materials [1]. For example, 1D nanobuilding blocks of transition metal oxides, hydroxides, sulfides, semiconductors, metals, and metal salts have now been prepared by various process

*Corresponding author. Email: sanand99@yahoo.com

Journal of Experimental Nanoscience
ISSN 1745–8080 print/ISSN 1745–8099 online
http://www.tandf.co.uk/journals
DOI: 10.1080/17458080601094421

techniques giving rise to the possibility of constituting a nanotoolbox for a "bottom-up" approach in nanoscience and nanotechnology [1–4]. Among the various materials mentioned above, semiconductor nanoscale materials, such as nanowires, nanorods, and nanodiscs have stimulated great interest due to their importance in basic research and potential applications [5]. They are quite attractive as components of electronic devices because many of their physical properties can be controlled through modification of the sizes and shapes of the building blocks [6, 7]. To this end, various techniques including the vapor-phase transport, laser ablation, chemical vapor deposition, arc-discharge, template-based, solution-chemistry methods, etc., have been developed to prepare well-aligned 1D nanomaterials [8–13]. However, it is still a challenge to develop simple methods for the fabrication of uniform nanomaterials that are cost-effective and allow large-scale production. Our main focus here is to review recent progress to establish convenient route (vapor–solid, vapor–liquid–solid, solid–liquid, etc.) to prepare robust semiconductor CuO nanostructured materials because this material has an advantage for application towards electronic and optoelectronic industry.

2. Preparation and characterization of CuO nanoparticles starting from the corresponding salts

In past decades, most of the research on synthesis of anisotropic nanocrystals has largely focused on II–IV semiconductor systems [14–20] other systems reported in the literature are very limited. Recently, copper-based nanomaterials have received attention because of their potential application in optoelectronic devices, catalysis and superconductors. CuO is a p-type semiconductor ($E_g = 1.2\,eV$) with excellent photovoltaic, electrochemical, and catalytic properties [21–24]. Also, it is inexpensive, non-toxic, and readily available.

Xu *et al.* [25, 26] reported the synthesis of CuO nanocrystals by one step solid state reaction under ambient conditions by grinding 2:5 molar ratios of $CuCl_2 \cdot 2H_2O$ and NaOH in an agate mortar followed by a short induction period of 30 min. The obtained black product was washed with an ultrasonic wave, distilled water (3 times), alcohol (2 times), and then dried in air. This method yielding polyhedral CuO nanocrystals with an average size of 12 nm was confirmed by TEM image (figure 1). XRD diffraction peaks (figure 2) also confirmed that the size of this CuO nanocrystal was found to be same by immediately pressing the powder as a pellet. Whereas an increase in grain size from 12.1 nm to 16.4 nm was observed on aging (15 days) of the pellet may be due to the more closely packed nanocrystals.

CuO belongs to the C_{2h}^6 space group shows three acoustic modes ($A_u + 2B_u$), six infrared active modes ($3A_u + 3B_u$), and three Raman active modes ($A_g + 2B_g$). Thus, the Raman spectra of CuO nanocrystal show three peaks at $282\,cm^{-1}$, $332\,cm^{-1}$ and $618\,cm^{-1}$ (figure 3). With aging, Raman peaks become sharper and show a slight blue shift because the grain size increases from 12.1 nm to 16.4 nm. From this study, it is concluded that there was change in the grain size only in the pressed pellets (due to their being more closely packed), not in CuO powder from XRD and Raman measurements.

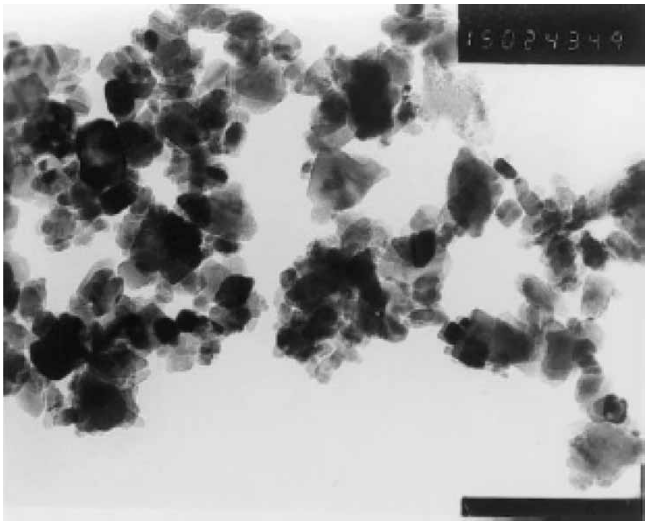

Figure 1. TEM micrograph of the CuO particles (×150,000) [25].

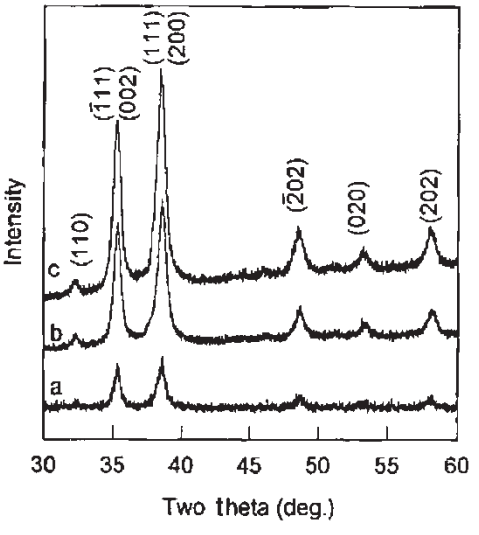

Figure 2. XRD curves of CuO pellet samples (a) just after pressed, (b) 4 days later, and (c) 15 days later at RT [25].

Wang *et al*. [27] prepared CuO nanowhiskers similar to Xu *et al*. [25] but in the presence of a nonionic surfactant. About 5.045 g of $CuCl_2 \cdot 2H_2O$ and 3 g of solid NaOH were ground for 5 min. To this mixture, 6 ml (6.78 g) of PEG 400 was added and the grinding continued for 30 min before washing the mixture several times with distilled water in an ultrasonic bath and then with ethanol to remove PEG 400, NaCl and unreacted precursors. Finally, the products were dried for 3 h in an oven at 60°C

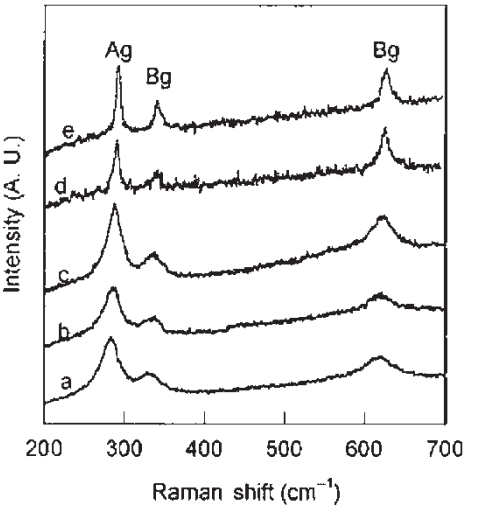

Figure 3. Raman spectra of CuO pellet samples (a) just after pressed, (b) 4 days later at RT, (c) 15 days later at RT, (d) annealed at 500°C for 2 h, and (e) annealed at 800°C for 2 h [25].

in air. The CuO nanowhiskers most likely form via the following reaction:

$$CuCl_2 \cdot 2H_2O(s) + NaOH \longrightarrow CuO(s) + 2NaCl + 3H_2O \quad (T = 298\,K)$$

The ionic liquid (PEG 400) exposes more ethyleneoxide monomers to the surface than in aqueous solutions which in due course interacts with water molecules to form a chain structure [28]. Thus, PEG 400 acts as a soft template leading to the formation of CuO nanowhiskers having an average size of ~8 nm in diameter and length scales larger than 100 nm (figure 4).

In addition, they also carried out preparation of CuO nanorods in the presence of nonionic surfactant [29] as follows. About 200 mg of PEG (M_w 20,000) and 178.48 mg of $CuCl_2 \cdot 2H_2O$ were dissolved in 200 ml of H_2O, which was stirred with a magnetic stirrer continuously until both the PEG and the $CuCl_2$ dissolved completely. Then 2 ml of NaOH solution (6 M) was added to the above mixture drop wise under constant stirring. While stirring $Cu(OH)_2$ blue precipitate formed which upon heating by steam for 30 min, generates CuO. The black CuO precipitate was washed several times with distilled water and then with ethanol to remove the PEG completely, filtered and dried in an oven at 80°C for 5 h. TEM image (figure 5) revealed that these materials have a relatively straight rod-like shape (diameters of ~10 nm and of length up to 400 nm) and smooth surfaces. The CuO lattice constants calculated for these nanorods by XRD data is consistent with the standard values of bulk CuO [30] and also results clearly indicate that the obtained nanorods were in fact crystalline CuO belonging to the monoclinic space group C_{2h}^6.

The CuO nanorods form here via two steps as shown below:

$$CuCl_2 + 2NaOH \longrightarrow Cu(OH)_2 + 2NaCl$$
$$Cu(OH)_2 \longrightarrow CuO + H_2O \quad (T = 373\,K)$$

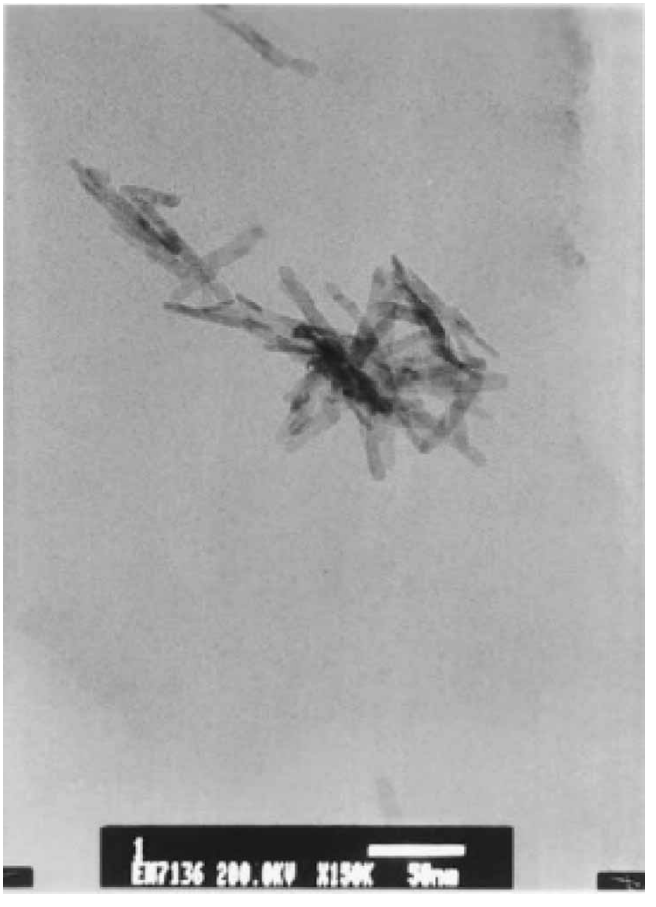

Figure 4. TEM image of the CuO nanowhiskers sample [27].

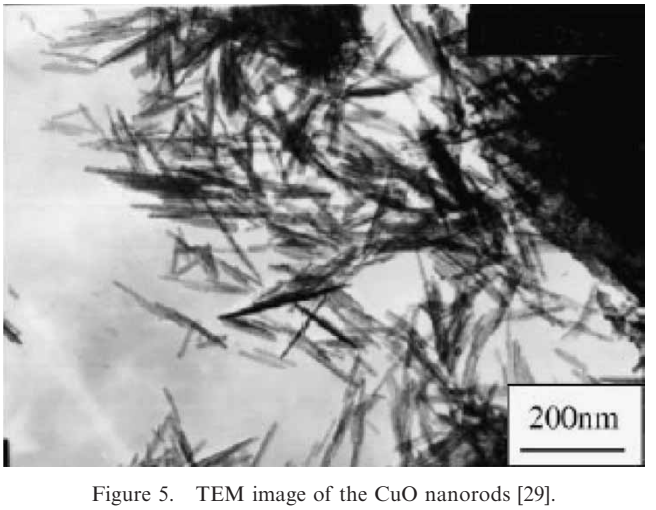

Figure 5. TEM image of the CuO nanorods [29].

Here also, the nonionic surfactant (PEG) acts as a template which plays an important role in controlling the CuO shape.

Similarly, Gao *et al*. [31] synthesized CuO nanorods starting from $CuCl_2$ as follows. First, $Cu(OH)_2$ precipitates were prepared by mixing 0.5 M solution of both $CuCl_2$ and NaOH. The obtained precipitates were dispersed in a 15 M NaOH solution of which one part of the dispersion was transferred into an autoclave with a PTFE container and kept at room temperature, while the second part was maintained at 100°C for 48 h. The obtained precipitates were washed in distilled water (until the solution pH ~ 7) and then dried at 100°C in air for 1 day. The average crystalline sizes of obtained CuO samples at room temperature and 100°C were estimated to be 17 nm and 73 nm from the XRD patterns (using Sherrer equation). The room temperature product was uniform fine nanorods of about 10–20 nm thick and several hundred nanometers long which are even thinner than the precursor $Cu(OH)_2$ precipitate (40–60 nm). Whereas at a temperature of 100°C, bulk CuO nanorods were obtained with a diameter 60–100 nm in size and length of up to 1 μm (figure 6). Thus, the morphological features of the synthesized

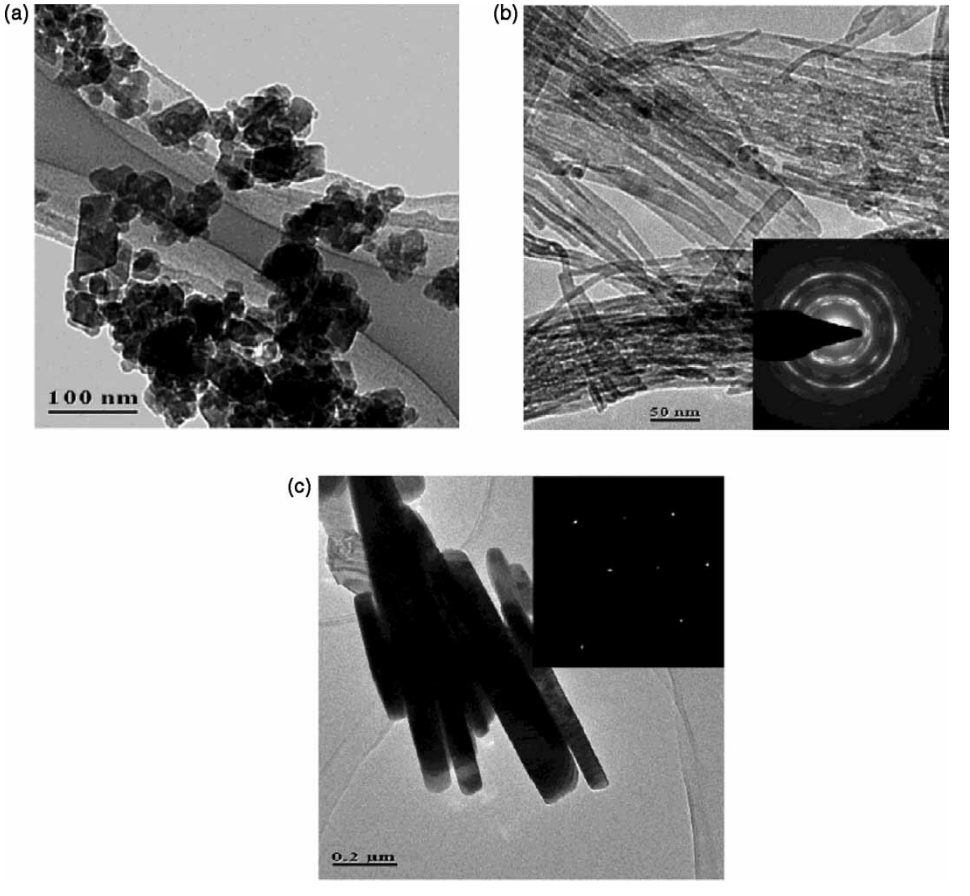

Figure 6. TEM images of $Cu(OH)_2$ precipitates dried at 100°C (a) and as-prepared nanorods at room temperature (b) and 100°C (c). The selected area electron diffraction of the as-prepared nanorods is inserted [31].

nanorods were highly dependent on temperature and caustic soda present in autoclaves. Also from the selected area electron diffraction (SAED) patterns it is concluded that bulk nanorods obtained at 100°C consist of single crystals while the fine nanorods obtained at room temperature have a polycrystalline structure (see inset of figure 6).

Secondly, Punnoose *et al*. [32] reported preparation of CuO nanoparticle by the sol-gel method. That is, mixing aqueous solutions of copper nitrate and sodium hydroxide at room temperature and by maintaining the pH $\sim$ 10. The resulting $Cu(OH)_2$ gel was washed several times with distilled water until free of nitrate ions, then centrifuged and finally dried in air. In order to get CuO nanoparticles, the $Cu(OH)_2$ gel obtained above was calcined in air for 3 h at the selected temperatures of 160, 200, 250, 300, 400, 600, 800 and 1000°C. The XRD patterns of the calcined samples (figure 7) show only lines due to CuO nanoparticles and also the particle size increases from 6.6 nm to 37 nm as the calcined temperature increases is determined by employing the Scherrer relation to the (202), (202) and (113) reflections [33]. The increase in grain size that may be due to the fusion of the particles on sintering is confirmed further by TEM micrographs (figure 8). That is, upon sintering small particles get aggregated and, in addition, the occurrence of surface faceting is evident from TEM micrographs.

Viano *et al*. [34] confirmed the agglomeration of nanoscale particles by TEM analysis (figure 9) while following the same synthesis procedure of Punnoose *et al*. [32]. They used electron spin resonance (ESR) technique to probe the calcination temperature effect on magnetic ordering in nano and bulk CuO powder. From the ESR results (figure 10), they concluded that (1) line shapes belong to typical polycrystalline material, (2) the appearance of broad signals are ascribed to weak antiferromagnetic ordering in CuO, and (3) the difference in line widths of the ESR

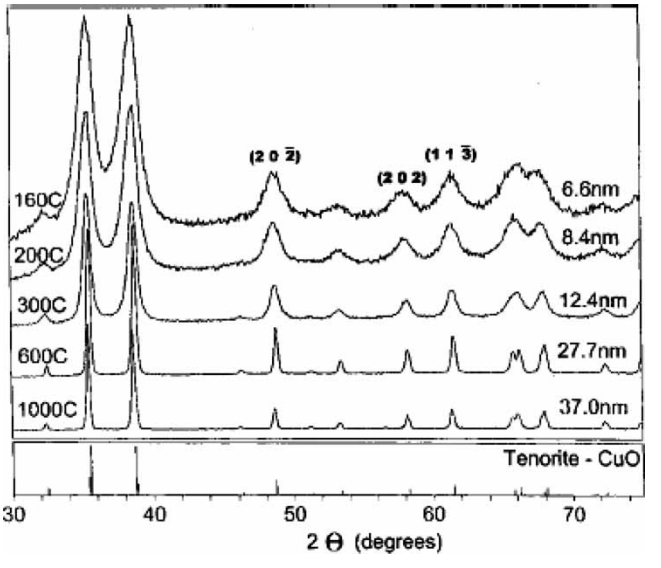

Figure 7. Room-temperature XRD patterns of CuO particles annealed at different temperatures shown. The particle size shown is the average value determined from the (20$\bar{2}$), (202), and (11$\bar{3}$) lines using the Scherrer relation, after correcting for the instrumental width. Temperatures are in °C [32].

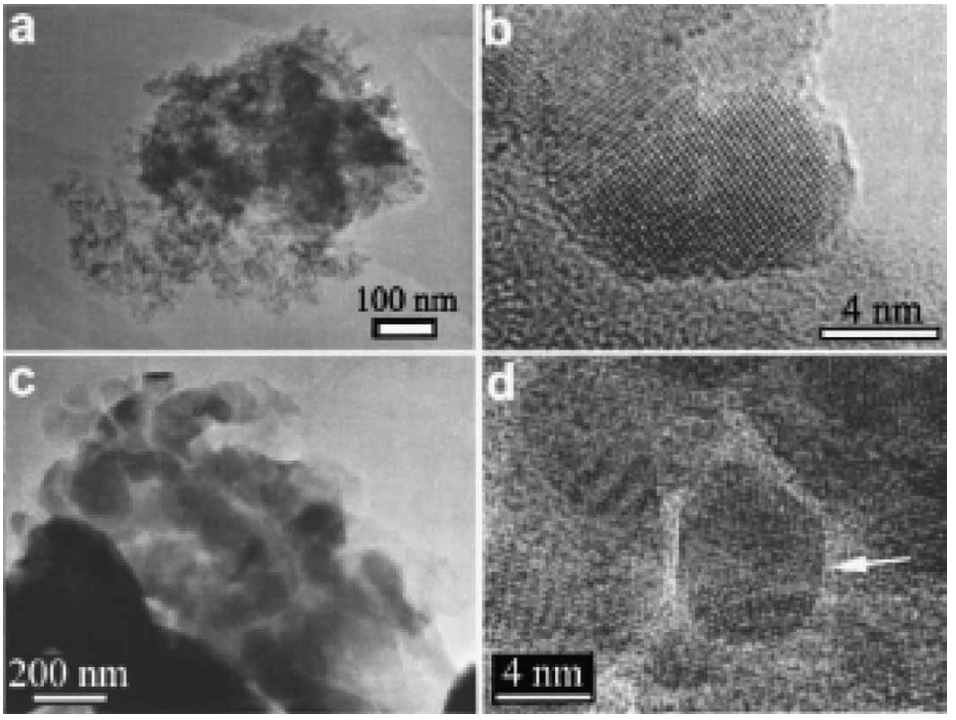

Figure 8. TEM characterization reveals agglomeration of the nanoscale particles. A cluster of 6.6 nm particles, shown in (a), consists of highly faceted single particles (b). A cluster of the nominal 33 nm particles is shown in (c). These large particles have surfaces decorated with smaller particles (d), which exhibit defects such as multiple twinning (arrow) [32].

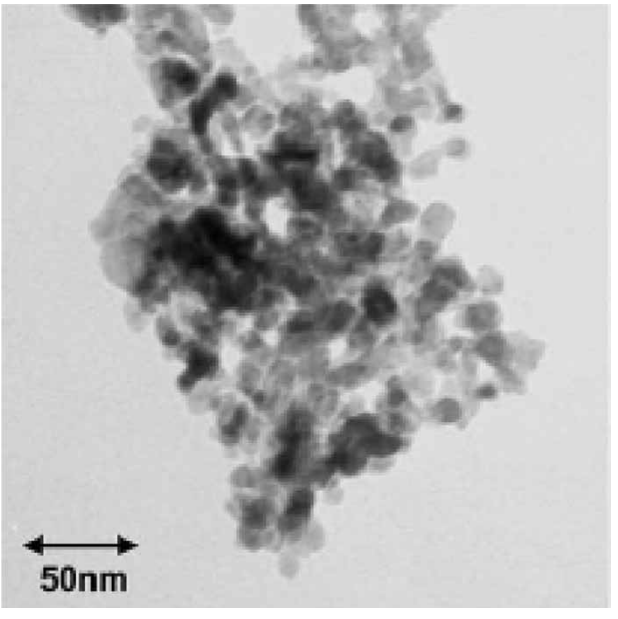

Figure 9. TEM image of CuO nanopowder calcined at 200°C [34].

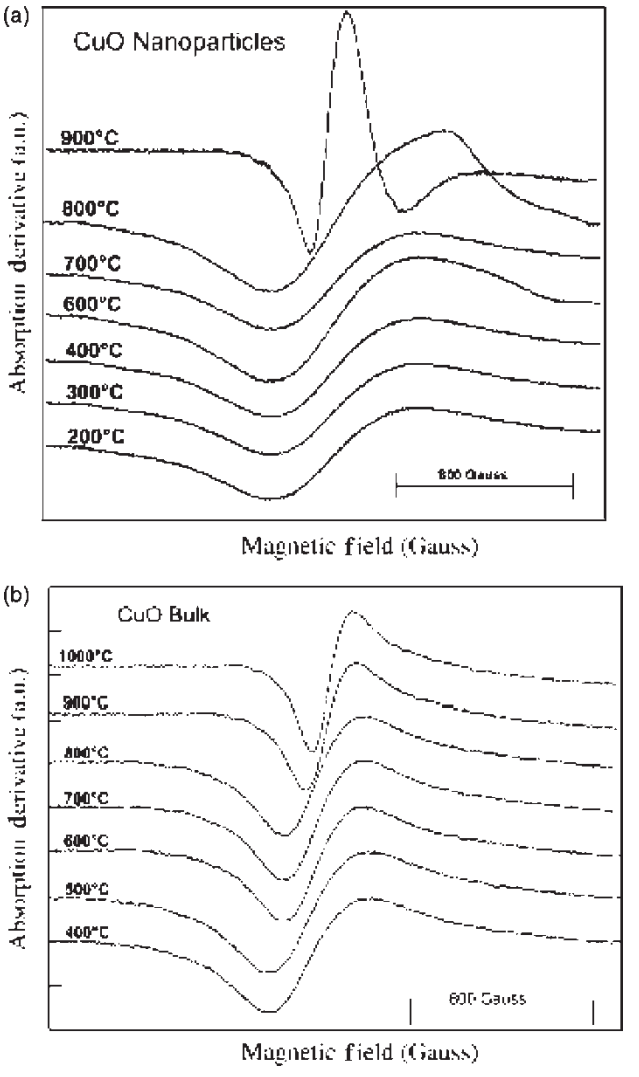

Figure 10. Overlay of ESR spectra of (a) CuO nanopowder and (b) CuO bulk calcined at different temperatures. The calcination temperature is written just above each curve [34].

signals between bulk and nanopowder indicates a high defect concentration in nanopowder, which must arise from the comparatively high surface area of nanoparticles. Thus the comparative study of bulk and nano CuO powder highlights the importance of particle size on the magnetic properties of nanoparticles.

Zhu *et al*. [35] reported preparation of CuO nanoribbons starting from $Cu_2Cl(OH)_3$ nanoribbons by template free method. First, $Cu_2Cl(OH)_3$ nanoribbons were prepared by mixing 1:2 molar ratio of $CuCl_2 \cdot 2H_2O$ and $(NH_4)_2CO_3$ solution and keeping the solution aside for 2–7 days. The jade-green precipitate formed was washed with distilled water and ethanol, and then dried at 60°C for 12 h yields $Cu_2Cl(OH)_3$ nanoribbons (see

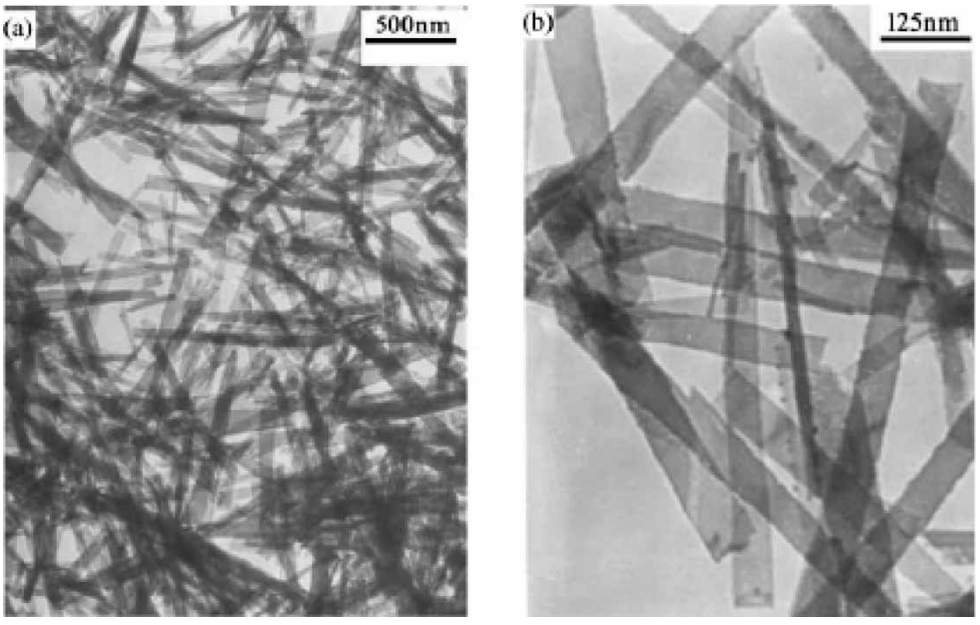

Figure 11. The TEM images of the $Cu_2Cl(OH)_3$ nanoribbon [35].

figure 11 for TEM image). The reaction that accounts for the formation of $Cu_2Cl(OH)_3$ nanoribbons probably proceed as follows:

$$
\begin{aligned}
(NH_4)_2CO_3 &\longrightarrow 2NH_4^+ + CO_3^{2-} \\
NH_4^+ + H_2O &\longrightarrow NH_3 \cdot H_2O + H^+ \\
CO_3^{2-} + H_2O &\longrightarrow HCO_3^- + OH^- \\
HCO_3^- + H_2O &\longrightarrow H_2CO_3 + OH^- \\
H_2CO_3 &\longrightarrow H_2O + CO_2 \\
Cu^{2+} + nNH_3 &\longrightarrow Cu[NH_3]_n^{2+} \\
Cu[NH_3]_n^{2+} + OH^- + Cl^- &\longrightarrow Cu_2Cl(OH)_3.
\end{aligned}
$$

In order to succeed in converting the $Cu_2Cl(OH)_3$ nanoribbon to CuO nanoribbon, the blue complex solution was transferred into a sealed Teflon-lined stainless-steel autoclave maintained at a relatively low temperature (105°C) so as to avoid the collapse of the ribbon morphology as much as possible. TEM image (figure 12) confirms the results for the conversions of $Cu_2Cl(OH)_3$ nanoribbon to CuO nanoribbon with an average width of 50 nm which corresponds well to the width of the sacrificial template. Also the SAED pattern confirms that the above-prepared CuO nanoribbons are polycrystalline (see inset of figure 12). Similarly, CuO nanostructures with nanoribbons, scroll-like structures etc. were prepared starting from single crystalline $Cu_2(OH)_2CO_3$ nanoribbons as precursors for sacrificial-template via heat treatments [36].

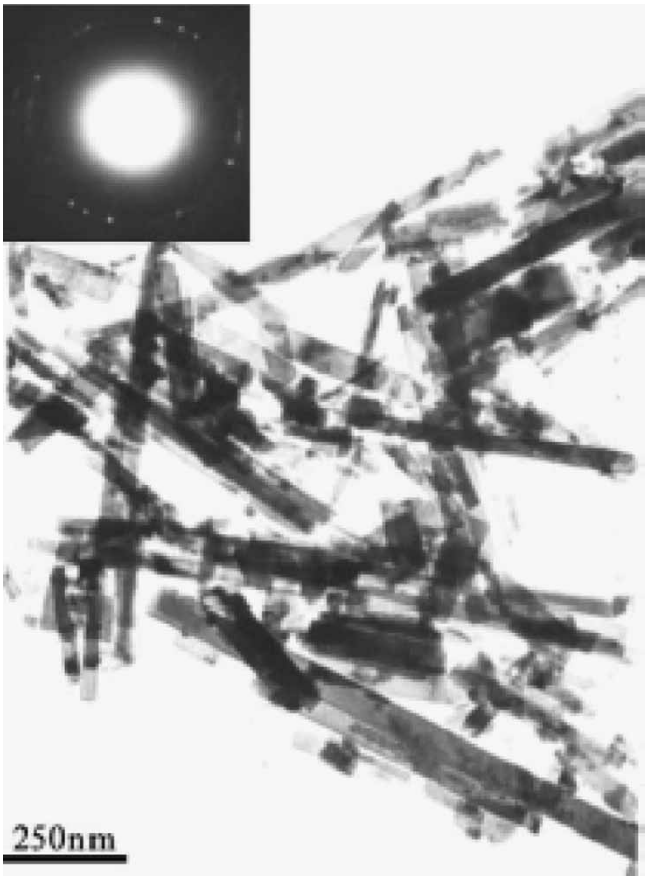

Figure 12. TEM image of CuO nanoribbon obtained by heat treatment of the $Cu_2Cl(OH)_3$ nanoribbon [35].

Song *et al*. [37] reported a different approach to the preparation for CuO nanowires starting from $Cu(DEHP)_2$ complex is as follows. First, $Cu(DEHP)_2$ complex were generated at pH 6 by mixing 2:1 molar ratio of bis(ethylhexyl) hydrogen phosphate (HDEHP) and $CuCl_2$ in heptane and water. Secondly, $Cu(OH)_2$ nanowire arrays were prepared at room temperature by injecting 20 ml of $Cu(DEHP)_2$ complex (0.05 M) in *n*-heptane into 20 ml of aqueous NaOH solution (0.05 M) taken in a 50 ml test tube. After several minutes, a blue colour gradually grew at the solution interface showing that the reaction occurs at the static organic/aqueous biphasic boundary. The product formed was taken out of the test tube after a given reaction time, washed with absolute alcohol, deionozied water, and dried in air. XRD and TEM analysis (figure 13) confirmed the formation of $Cu(OH)_2$ nanowires at the interface. Finally, black CuO nanowire arrays (figure 14) were obtained by allowing the above reactions to take place at (i) higher concentration of NaOH and (ii) more reaction time.

Lu *et al*. [38] reported a simple template-free solution route for the controlled synthesis of $Cu(OH)_2$ and CuO nanostructures starting from $CuSO_4$ solution.

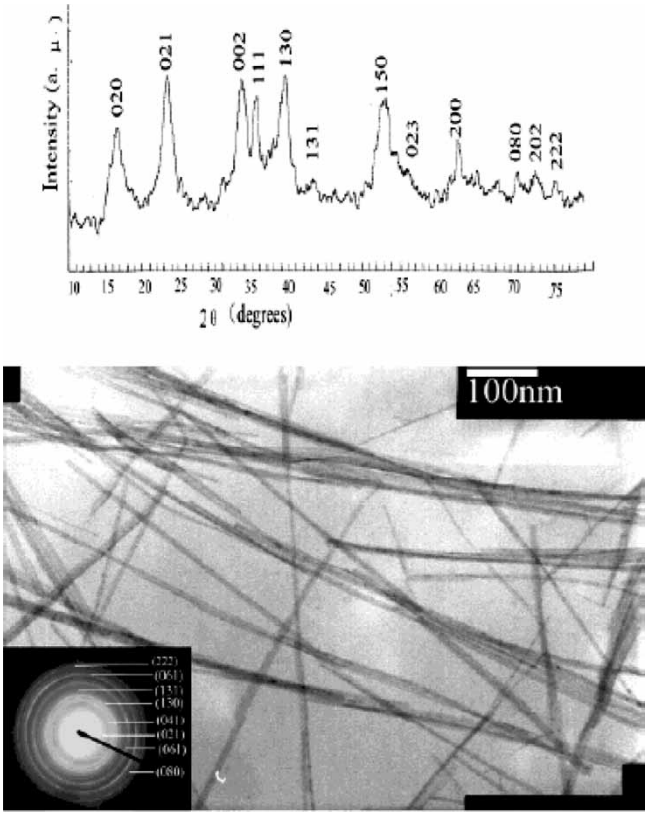

Figure 13. XRD and TEM image of $Cu(OH)_2$ prepared at the static interface between $Cu(DEHP)_2 = 0.05$ M in *n*-heptane and NaOH = 0.05 M [37].

They followed two different methods for the synthesis of $Cu(OH)_2$ nanostructures, i.e., the KOH/NH_3 route and the NH_3/KOH route. In the first route (KOH/NH_3), about 0.8 ml of KOH solution (1M) was added into 2 ml of $CuSO_4$ solution (0.1 M) under rigorous stirring at ambient temperature followed by addition of 0.3 ml of ammonia solution (12.5 wt%, ~7.0 M). Further stirring the sample for a while and then kept mixed solution static in a sealed vessel for 12 h followed by filtering, washing thoroughly with deionized water and dried in a vacuum at 25°C for 12 h generates $Cu(OH)_2$ nanowires (figure 15). For the second route (NH_3/KOH), the synthesis procedures are same but the feeding order of NH_3 and KOH are vice-versa compared to the first method. For this method $Cu(OH)_2$ nanoribbons were obtained which was confirmed by SEM and TEM images (figure 16). The exact reactions for the selective formation of $Cu(OH)_2$ nanowires and nanoribbons are as follows:

(a) KOH/NH_3 route

$$Cu^{2+} + OH^- \longrightarrow Cu(OH)_2 \cdot H_2O \xrightarrow[\text{Coordination self-assembly, oriented attachment}]{NH_3 \cdot H_2O} \underset{\text{(nanowires)}}{Cu(OH)_2}$$

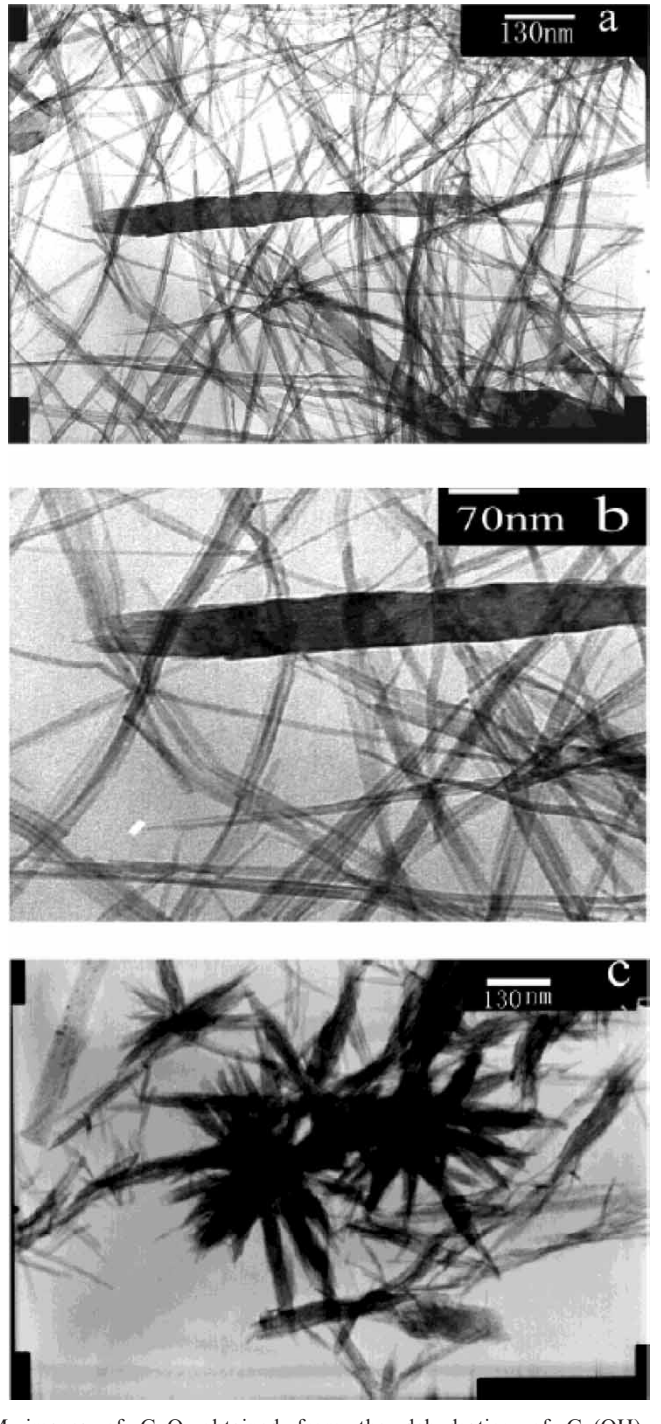

Figure 14. TEM images of CuO obtained from the dehydration of $Cu(OH)_2$ at the different concentrations of NaOH (a) and (b) $Cu(DEHP)_2 = 0.05\,M$ and $NaOH = 0.1\,M$ at different magnifications. (c) $Cu(DEHP)_2 = 0.05\,M$ and $NaOH = 0.2\,M$ [37].

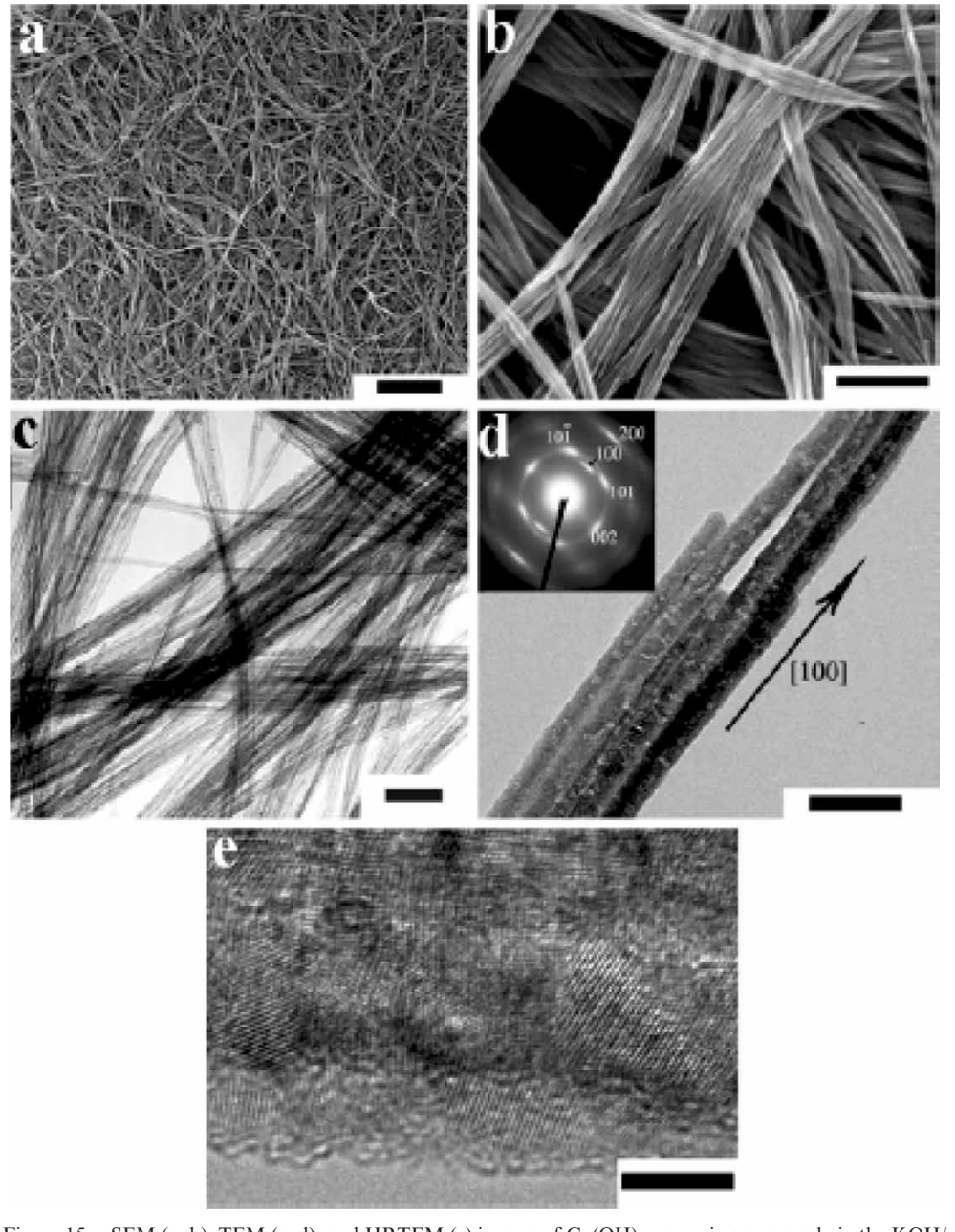

Figure 15. SEM (a, b), TEM (c, d), and HRTEM (e) images of $Cu(OH)_2$ nanowires prepared via the KOH/NH_3 route aged for 12 h. Inset shows ED pattern of the bundled nanowires. Scale bars: (a) 5 μm; (b) 500 nm; (c) 100 nm; (d) 50 nm; (e) 5 nm [38].

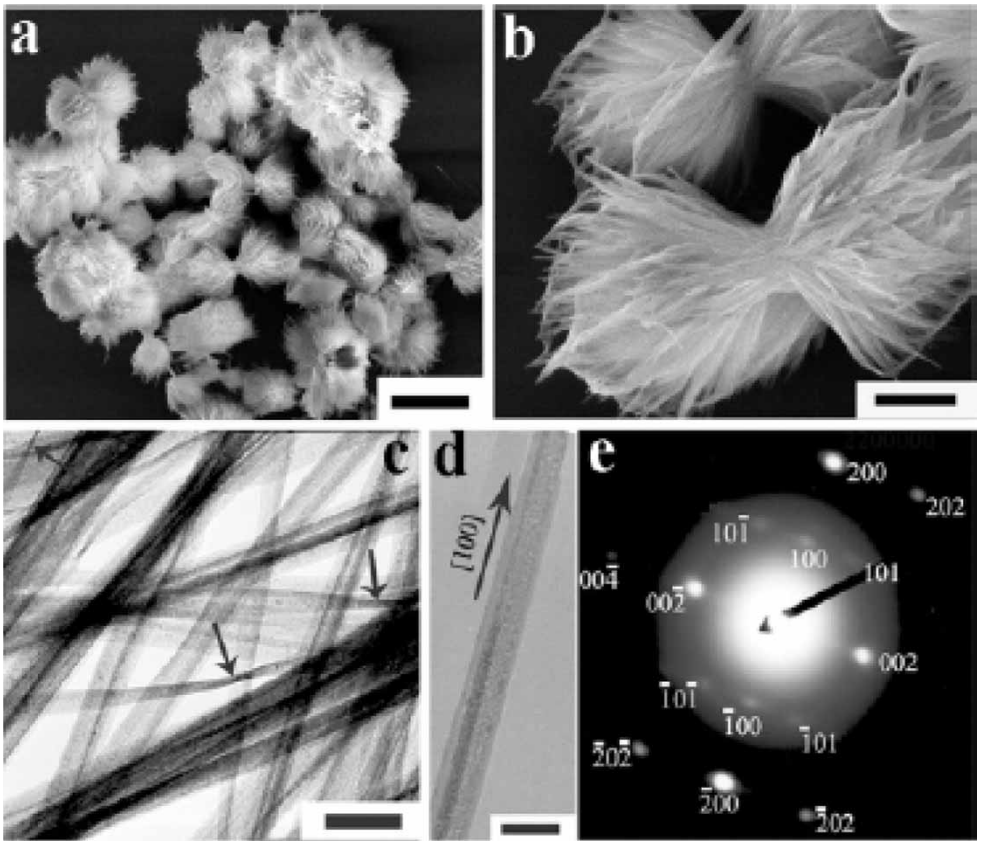

Figure 16. SEM (a, b) and TEM (c, d) images and ED (e) patterns of $Cu(OH)_2$ nanoribbons prepared via the NH_3/KOH route. The ED pattern shown in plate e corresponds to the single nanoribbon shown in plate d. Scale bars: (a) 5 μm; (b) 1 μm; (c) 200 nm; (d) 100 nm [38].

(b) NH_3/KOH route

$$Cu^{2+} + NH_3 \cdot H_2O \longrightarrow [Cu(NH_3)n]^{2+} \xrightarrow[\text{Coordination self-assembly}]{OH^-} \underset{\text{(nanoribbons)}}{Cu(OH)_2}$$

The thermal dehydration of the 1D $Cu(OH)_2$ nanowires obtained through KOH/NH_3 route in the solution phase generates CuO nanoplatelets (figure 17), upon heating the original solution below 50°C after the addition of the two alkaline solutions, and aged at 50°C. But for the 1D $Cu(OH)_2$ nanostructures only bundles of CuO nanowires (figure 18) were obtained without any change in the morphology, when dehydrated the sample in the solid state at 120°C for 2 h. While, for the $Cu(OH)_2$ nanoribbons synthesized via NH_3/KOH route, a unique flower like aggregates consisting of CuO nanopetals (figure 19) were obtained, when the $Cu(OH)_2$ nanoribbons were dispersed in water and heated at 70°C for 12 h.

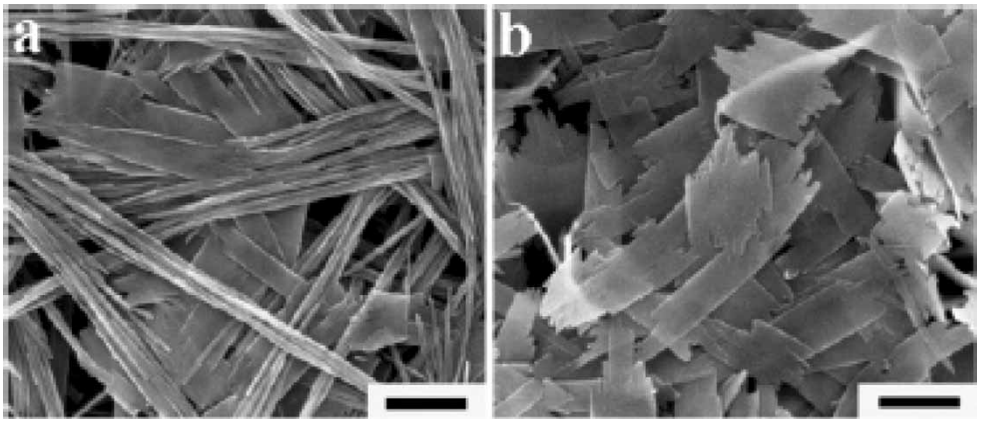

Figure 17. SEM images (a, b) of CuO nanoplatelets obtained by thermal dehydration of the $Cu(OH)_2$ nanowires prepared via the KOH/NH_3 route immediately after the addition of the KOH and ammonia solutions: (a) 30°C; (b) 50°C. Scale bars: 500 nm [38].

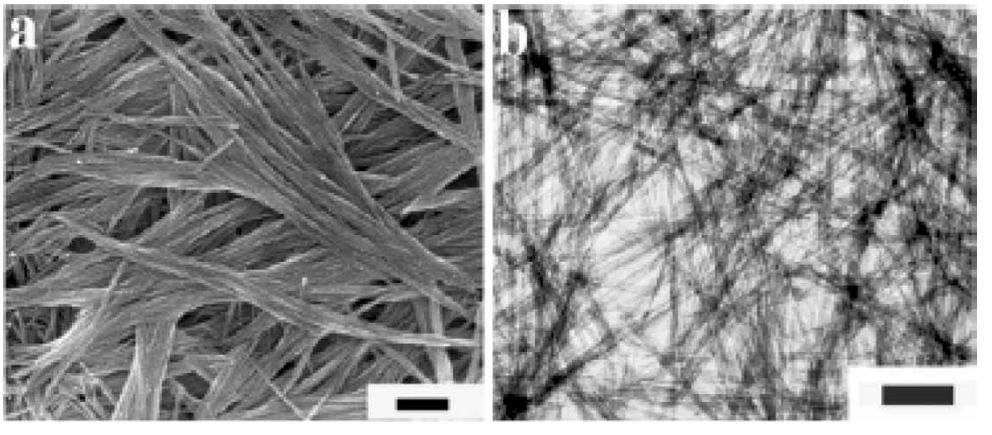

Figure 18. SEM (a) and TEM (b) images of CuO nanowires obtained by thermal dehydration of the as prepared $Cu(OH)_2$ nanowires in the solid state at 120°C for 2 h. Scale bars: (a) 500 nm; (b) 200 nm [38].

Zeng *et al.* [39] reported synthesis of CuO nanorods and nanoribbons by wet chemical method in which water–ethanol mixture is used as a solvent. 40 ml of $Cu(NO_3)_2 \cdot 3H_2O$ (0.01 M in pure ethanol) was slowly added at a rate of 0.1 ml/min using a mechanically pumped syringe to 40 ml of NaOH (0.5 M in ethanol) solution under stirring in a Teflon flask at 65°C and the resultant product was then aged together with mother liquor at the same temperature for 12–36 h respectively. Separation of CuO nanocrystals were done by centrifugation at a speed of 6000 rpm for 10 min followed by washing with de-ionized water repeatedly and then dried under vacuum overnight at room temperature. In addition, they found that the dimensions of the nanostructured CuO can be controlled across a wide spatial span from nanometer to micrometer regime via manipulating synthetic parameters (summarized in table 1)

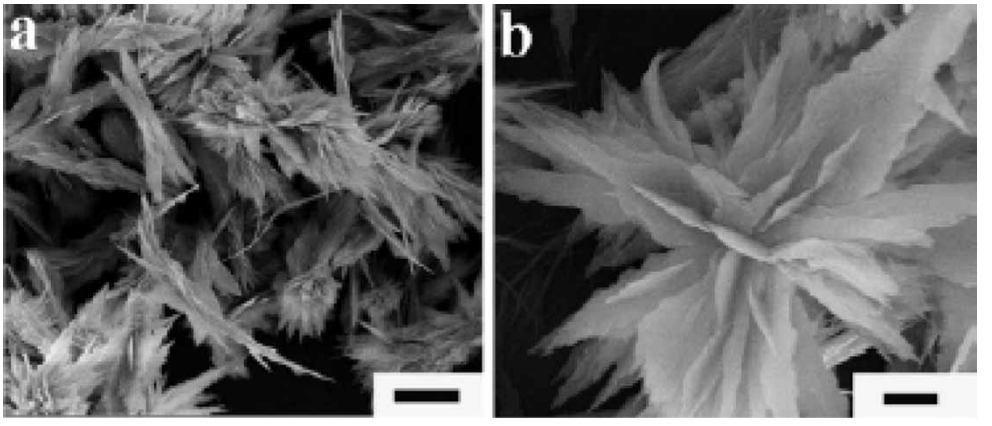

Figure 19. SEM images of CuO nanostructures obtained by thermal dehydration of the as prepared $Cu(OH)_2$ nanoribbons in water at 70°C for 12 h. Scale bars: (a) 2 μm; (b) 500 nm [38].

and most importantly desired morphology of CuO crystallites (rod, wire, ribbon, net, platelet or sheet) can be obtained by selecting simple changes of reaction conditions. To achieve this, NaOH is playing a number of roles in the synthesis. First it combines with $Cu(NO_3)_2$ to form $Cu(OH)_2$, which is then decomposed to CuO as follows:

$$Cu(NO_3)_2 \cdot 3H_2O + 2NaOH \longrightarrow CuO + 2Na(NO_3)_2 + 4H_2O$$

Since, heating was used to accelerate the reaction, no $Cu(OH)_2$ intermediate precipitate was observed. Secondly, NaOH is a strong electrolyte, and it may neutralize the surface charges of the CuO nanorods, preventing them from possible crystallite aggregation. Finally, the high concentrated NaOH used may create diffusion layers on certain surfaces of CuO nanorods, which may create an additional growth anisotropy allowing only energetically favourable crystallographic planes to grow. Thus, from the simple wet-chemical methods the following points to be noted: (1) at low reaction temperatures and normal atmospheric pressure, single crystalline monodispersed CuO nanorods with a selected breadth in the range of 5–15 nm can be prepared by simply changing the starting copper ion concentration, (2) upon the ageing treatment, morphology of the CuO nanorods can be further modified, and (3) nanoplatelets or sheets of CuO can also be synthesized with a high concentration solution of NaOH.

In addition, they reported how CuO crystallites self-organized into spherical assemblies or "dandelions" with a puffy appearance (figure 20) [40]. The synthesis procedure for such samples is as follows: About 15–25 ml of $Cu(NO_3)_2 \cdot 3H_2O$ (1 M in pure ethanol solvent) was added to 15–25 ml of ammonia solution (32%), followed by an addition of 4–5 ml of aqueous NaOH (1 M) and 0–5 g of solid $NaNO_3$. The solution mixture was then transferred to a Teflon-lined stainless steel autoclave and heated at 100–180°C for 2–24 h in an electric oven. After reaction, the autoclave was cooled in tap water, and CuO products were washed via centrifugation-redispersion cycles, with each successive supernatant being decanted and replaced with deionized water and ethanol.

Table 1. Experimental procedures and product results [39].

Expt	Preparation procedure	Result
A	40 mL of NaOH (0.5 M[a]) + 40 mL of Cu^{2+} (0.01 M[a]) at 0.1 mL/min and 65°C, aged for 12–36 h	Amorphous product
B	40 mL of NaOH (0.5 M[a]) + 40 mL of Cu^{2+} (0.01 M[a]) at 0.1 mL/min and 77°C + 40 mL of H_2O at 0.2 mL/min and 77°C, aged for 0–60 h	Short nanorods, breadth = 5–8 nm
C	40 mL of NaOH (0.5 M[a]) + 40 mL of Cu^{2+} (0.03 M[a]) at 0.2 mL/min and 78°C + 60 mL of H_2O at 0.1 mL/min and 78°C, aged for 0–126 h	Short nanorods, breadth = 8–10 nm
D	20 mL of NaOH (0.5 M[a]) + 20 mL of Cu^{2+} (0.08 M[a]) at 0.1 mL/min and 78°C + 40 mL of H_2O at 0.1 mL/min and 78°C, aged for 0–16 h	Short nanorods, breadth = 10–15 nm
E	20 mL of NaOH (0.5 M[a]) + 20 mL of Cu^{2+} (0.01 M[a]) at 0.2 mL/min and 81°C + 20 mL of H_2O, aged for 3 h; then 40 mL of NaOH (0.5 M[a]) + 40 mL of Cu^{2+} (0.02 M) both at 0.1 mL/min and 81°C, aged for 0–39 h	Long nanoribbons, breadth = 5–15 nm, long nanorods (after aging)
F	40 mL NaOH (5 M[b]) + 40 mL Cu^{2+} (0.02 M[b]) at 0.1 mL/min and 82°C + 40 mL Cu^{2+} (0.02 M[b]) at 0.3 mL/min and 82°C, during which 16 g of NaOH was also added, aged for 0–90 h	Nanoribbons, nanoplatelets, nanosheets (maximum area = 500 × 1000 nm)

[a]In pure ethanol; [b]in deionized water.

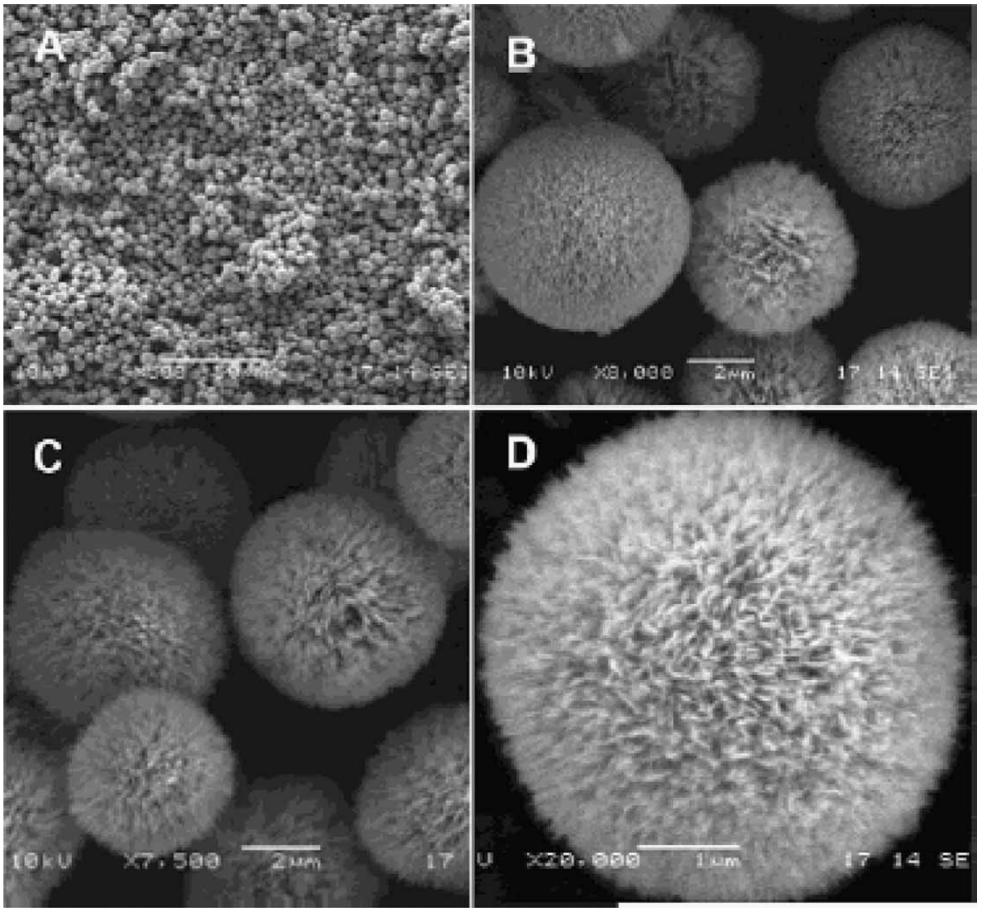

Figure 20. SEM images of CuO microspheres (prepared at 100°C, 24 h): (a) overall product morphology; (b and c) detailed views on average sized spheres; and (d) a detailed view on an individual sphere [40].

Under the reported conditions, the prepared CuO products are all in the "dandelion"-like morphology (100%), with diameters ranging from 4–8 μm.

3. Preparation and characterization of CuO nanoparticles starting from the corresponding acids

In past decades, much effort has been made towards the synthesis and characterization of nanosized transition metal oxide particles. Among all transition metal oxides that have been investigated, much less time has been devoted to the preparation and characterization of CuO nanoparticles. For example, Yang and Gao [41] reported preparation of CuO nanocrystals with various morphologies via a simple and convenient hydrothermal decomposition route. That is, by mixing about 0.5 g of $Cu(COOH)_2$ in a series of mixture of anhydrous dimethyl sulphoxide (DMSO) and

distilled water (total volume 70 ml and volume ratios were 50:3, 10:1, 5:1, 5:2 and 1:1) in a Teflon-lined autoclave. The whole mixture was then maintained at 110°C for 3 h and cooled to room temperature naturally yields CuO nanocrystals. The obtained CuO black precipitates were collected and washed with distilled water followed by absolute ethanol several times. The final products were dried in vacuum at 60°C for 6 h.

The following reactions supported such preparation methods.

$$\mathrm{D + H{-}O{-}H \rightleftharpoons [D{-}H]^+ + OH^-} \quad \text{(where D = DMSO)}$$
$$\mathrm{Cu(COOH)_2 + 2OH^- \longrightarrow Cu(OH)_2 + 2COOH^-}$$
$$\mathrm{Cu(OH)_2 \longrightarrow CuO + H_2O}$$

From the TEM photographs (figure 21), it is concluded that morphology of CuO nanocrystals changes from spherical to leaf like morphology via nanorod structures with the increase of water in the reaction. This is because the surface tension of the DMSO–H_2O mixtures increases with water content [42]. When the water content is low, the DMSO tends to absorb the water vapor more quickly which results in abundant small nuclei of CuO. In addition, DMSO acts as a dynamic stabilizer [43], whose molecules can be bound to the surface of the nuclei through donating a lone pair of electrons from oxygen atom to the empty orbitals of the copper atoms, which tend to hinder the more combinations of Cu^+ and OH^-. Further, the steric effect caused by the DMSO molecules and the generation of more OH^- with the increase of water content (identified from the pH value) can also limit the growth of the nuclei.

Xu *et al.* [44] reported preparation of CuO nanorods by thermal decomposition of CuC_2O_4 similar to Yang and Gao [41] but they use copper acetate, oxalic acid and surfactant (nonyl phenyl ether) as starting compounds. That is, about 3.99 g of $Cu(CH_3COO)_2 \cdot H_2O$ and 2.53 g of $H_2C_2O_4 \cdot 2H_2O$ were mixed with 5 ml of nonyl phenyl ether 9/5 (NP-9/5) in a mortar, grind for several minutes and kept in a thermostat oven at 50–60°C for 6 h. Then the product was washed several times with distilled water and acetone to remove unreacted reactants and then dried in an oven at 70–80°C for 12 h to yield pure CuC_2O_4. To yield CuO nanorods, grind about 2 g of CuC_2O_4 as synthesized above with 8 g of NaCl powder, and then annealed at 950°C for 2 h in a porcelain crucible. Finally, the annealed sample was washed with distilled water one time, ethanol three times, ethyl ether one time using an ultrasonic bath and then centrifuge to yield CuO nanorods. TEM morphologies (figure 22) confirmed the as-synthesized CuO nanorods were around 30 nm in diameter and length of several micrometers. The existence of conical tip at the end of nanorod conforms that the growth mechanism of the CuO nanorods is most likely controlled by the vapour-solid (VS) growth mechanism.

The following reactions supported such preparation methods.

$$\mathrm{C_2O_4^{2-} + Cu^{2+} \longrightarrow CuC_2O_4}$$
$$\mathrm{CuC_2O_4 \longrightarrow CuO + CO + CO_2}$$

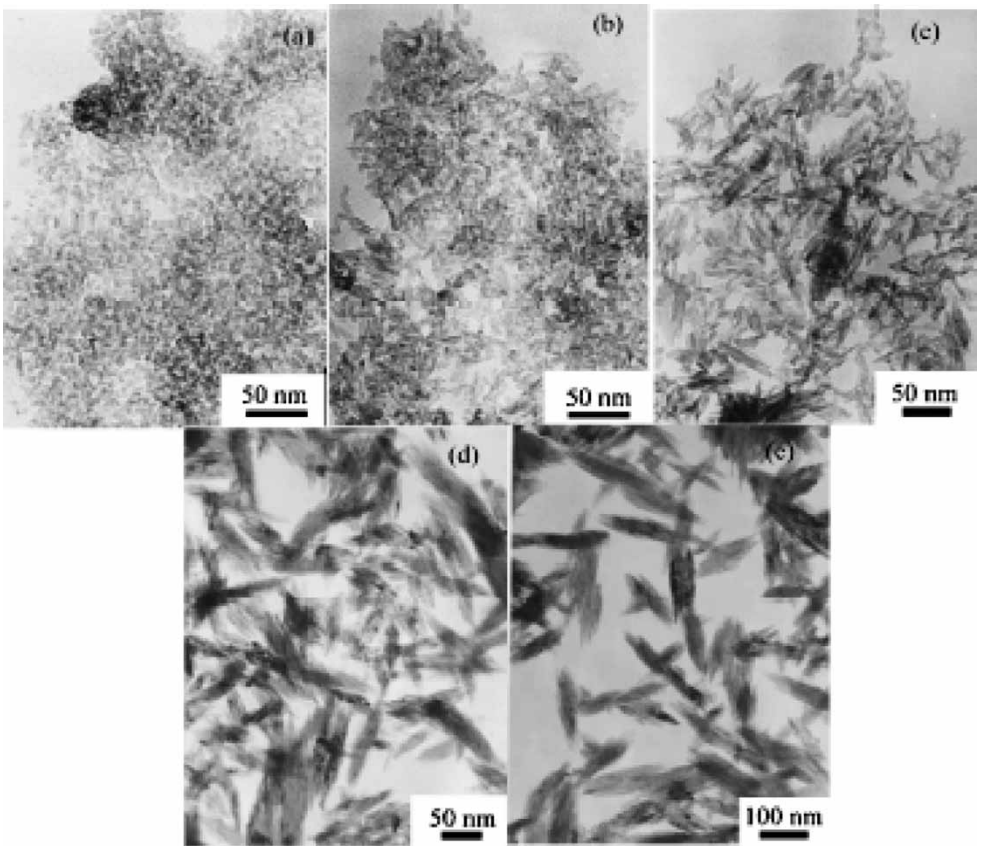

Figure 21. Representative TEM images of CuO nanocrystals synthesized at various volume ratios of DMSO and water: (a) 50:3; (b) 10:1; (c) 5:1; (d) 5:2; (e) 1:1 [41].

The use of surfactant may act as a template to form fine particle and also provide a favorable environment for the growth of CuO nanorods, i.e., make a ''shell'' surrounding the particles to prevent them from aggregating to larger particles during the grinding process.

Hong *et al.* [45] also followed alcohothermal route to synthesize CuO nanoparticles starting from copper acetate. That is 50 ml of copper acetate alcoholic solution (0.05 M) was taken in a Teflon lined stainless steel autoclave and kept constant in an oven at various temperatures (90°C, 110°C, 130°C, 150°C and 180°C) for 20 h. After cooling the autoclave to room temperature, the products were recovered by centrifugation, washed with distilled water (twice), ethanol (three times) and then vacuum dried at room temperature. Through this approach, stable CuO nanoparticles as small as 3–9 nm have been successfully synthesized below 150°C. However, the rate of formation of CuO nanoparticle was slow when the synthesis temperature was below 90°C and on the other hand, if the temperature was raised above 180°C, reducing alcohol would readily reduce the Cu(II) to metallic copper nanoparticles with a relatively large size of 54.1 nm. This may be confirmed from the XRD patterns (figure 23).

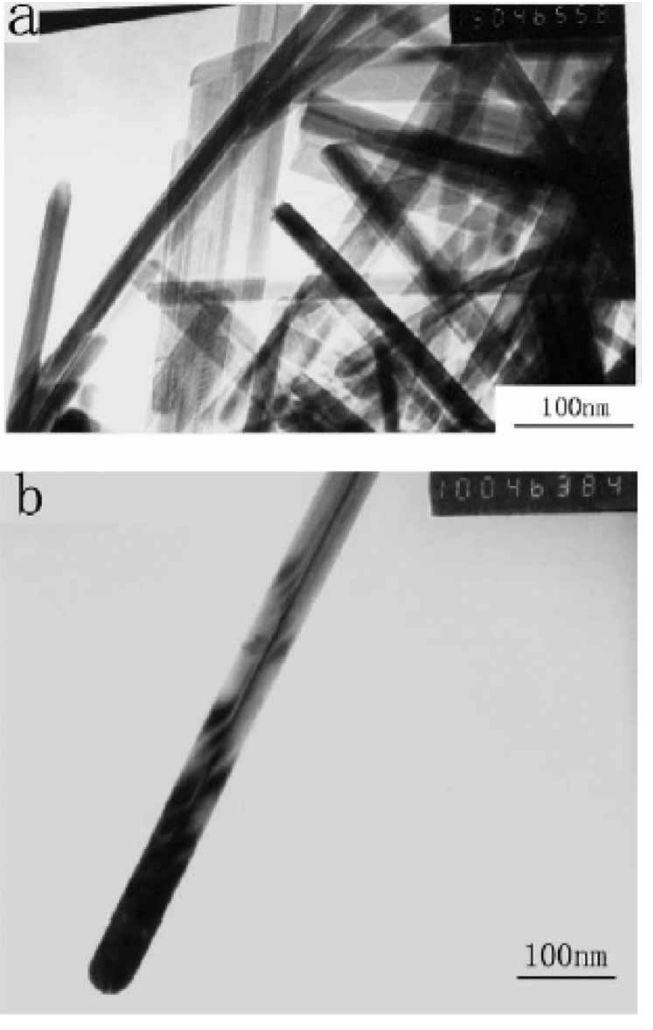

Figure 22. TEM images of the as-prepared CuO nanorods. (a) Morphologies of the as prepared CuO nanorods. (b) Morphologies of the as prepared single CuO nanorod [44].

Similarly, Wang *et al*. [46] reported synthesis of CuO nanoparticles by microwave irradiation of copper acetate. About 25 ml ethanolic solutions of both copper acetate (0.2 M) and NaOH (0.01 M) were taken in a round-bottomed flask with 0.5 g of polyethylene glycol −19,000 (PEG). The reaction was carried out under ambient air by keeping the total mixture under microwave irradiation. The microwave oven followed a working cycle of 6 s on and 24 s off and altogether the on/off heating procedure was repeated 20 times. After cooling the irradiated mixture to room temperature, the products were recovered by centrifugation, washed with distilled water, absolute ethanol and acetone, and then dried in air at room temperature.

By this microwave irradiation approach, the size of the CuO particles obtained can be in the range of 3–5 nm (figure 24) with the presence of dispersant (PEG). While in the

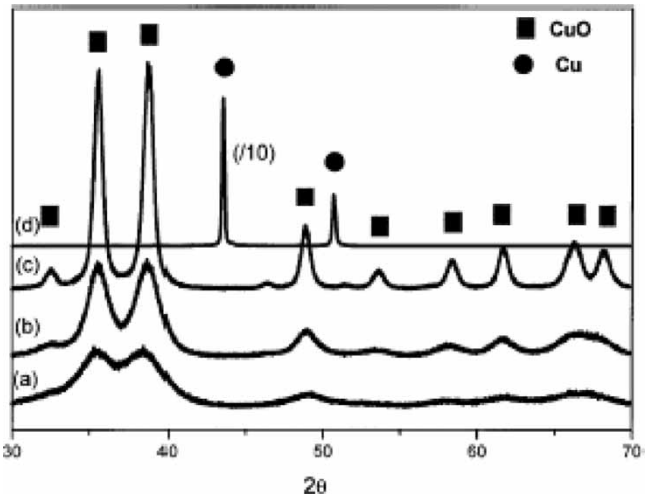

Figure 23. X-ray diffraction patterns of the samples prepared using the alcohothermal route at different temperatures: (a) 90°C; (b) 110°C; (c) 150°C; and (d) 180°C [45].

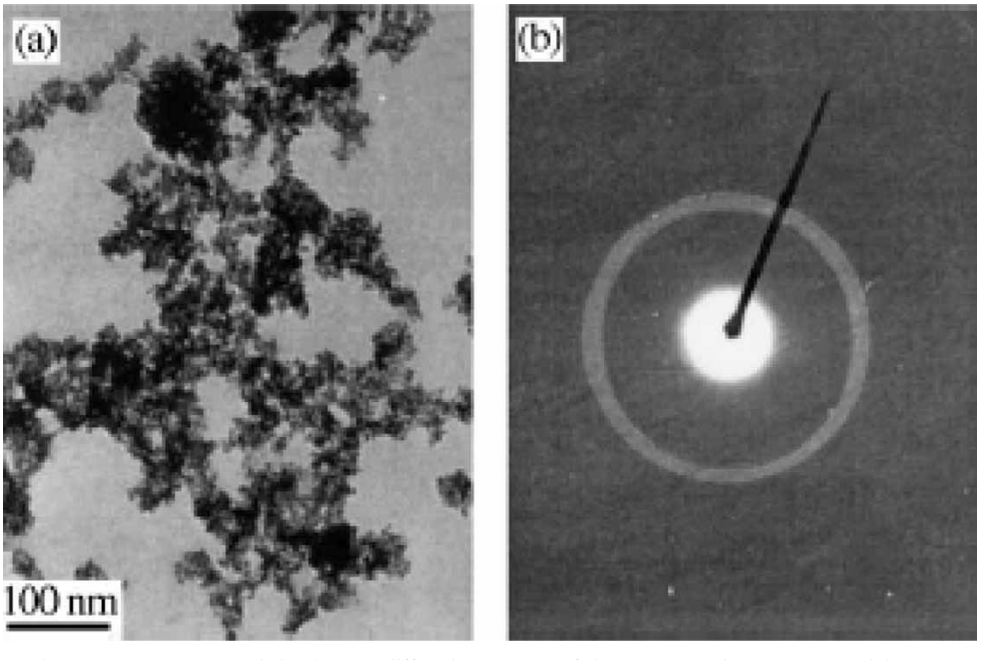

Figure 24. (a) TEM and (b) electron diffraction pattern of the as-prepared CuO nanoparticles [46].

absence of dispersant (PEG), CuO nanoparticles get agglomerated to form some quadrate aggregates of over 200 nm (figure 25). These can be explained by the stabilization effect of the surface caused by PEG. That is, the existence of dispersant PEG may reduce the Gibbs's free energy at the surface of the CuO nanoparticles and

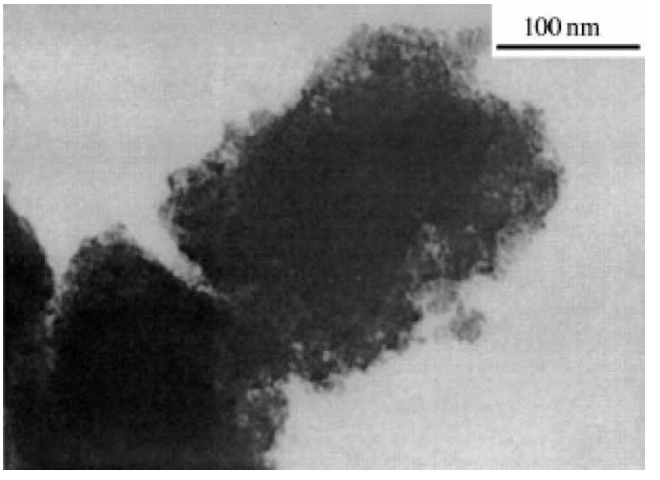

Figure 25. TEM image of the CuO nanoparticles prepared in the absence of PEG [46].

thus prevent the grains from merging into larger ones. The mechanism for this approach is proposed similar to Iwasaki *et al.* [47] as follows.

$$\mathrm{NaOH + EtOH \rightleftharpoons EtONa + H_2O}$$

$$\mathrm{CuAc_2 + EtONa \longrightarrow EtO{-}Cu{-}Ac + NaAc}$$

$$\mathrm{Eto{-}Cu{-}Ac \xrightarrow{H_2O} Ac{-}Cu{-}OH}$$

$$\mathrm{2Ac{-}Cu{-}OH \xrightarrow{-H_2O} Ac{-}Cu{-}O{-}Cu{-}Ac}$$

$$\mathrm{Ac{-}(Cu{-}O)Cu{-}Ac \xrightarrow[\text{irradiation}]{\text{microwave}} CuO + CuAc_2}$$

That is, nucleophilic attack by ethoxide produces an intermediate (EtO–Cu–Ac), which on hydrolysis produces another intermediate (Ac–Cu–OH). Cu–O–Cu bonds were formed by dehydration-condensation of this intermediate followed by decomposition leads to CuO nanoparticles under microwave irradiation.

4. Preparation and characterization of CuO nanoparticles starting from the corresponding metal

Apart from the routine method of synthesis of CuO nanoparticles starting from their corresponding salts, there are also reports [1] available on syntheses of CuO nanoparticles from the corresponding metal. For example, Borgohain *et al.* [48] prepared stable CuO nanoparticles having size as small as 4 nm by novel electrochemical route using a copper metal electrode as sacrificial anode and platinum as cathode in an electrochemical bath comprised of tetraoctylammonium bromide

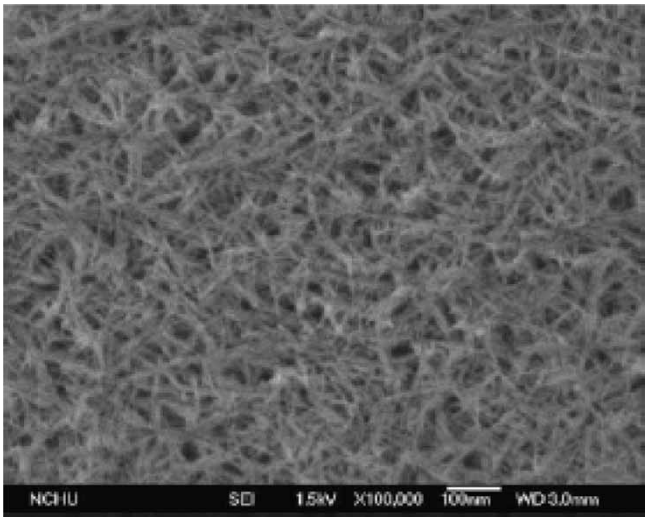

Figure 26. SEM image of the CuO nanoparticle [49].

(TOAB) in acetonitrile and tetrahydrofuran, in the ratio 4:1 as electrolyte. This method gives a high yield of sample, without any undesired side products compared to the synthetic routes involving corresponding salts as their starting material.

Secondly, Lo *et al*. [49] reported preparation of CuO nanofluid by submerged arc nanoparticle synthesis system (SANSS) using a copper electrode. A pure copper rod is deployed to prepare nanoparticles, submerged in dielectric liquid (deionized water) in the vacuum chamber. By generating an electric arc at high temperature (between 6000–12,000°C), the rod is melted and vaporized, undergoing nucleation, growth and condensation in the submerged deionized water to disperse nanoparticles. The morphology of the CuO nanoparticle prepared by this method revealed a needle-like structure (figure 26) with an average width of 20 nm and length of 80 nm.

In the late 1950s, Nabarro and Jackson [5] reported preparation of CuO and Cu_2O nanowhiskers of short length (<5 μm) and large diameter (>100 nm) by oxidizing copper substrate. But recently, Jiang *et al*. [50] reported preparation of CuO nanowires of controllable diameter in the range of 30–100 nm with lengths of up to 15 μm by simply heating copper foils at different temperature and growth time. They followed the procedure as follows: First, the copper substrate was cleaned in an aqueous 1 M HCl solution, followed by repeated rinsing with distilled water. After it had been dried under a N_2 gas flow; it was placed in an alumina boat and immediately heated to the set-point temperature (at ambient pressure) in a furnace. The surfaces of the copper substrates were tarnished (when viewed by the naked eye) after they had been treated in air at elevated temperatures. Further examination of the sample under optical or electron microscope indicated the formation of wire-like nanostructures over the entire surfaces of these substrates. For example, TEM images (figure 27) conclude that the diameter of the CuO nanowires could be varied in the range of 30–100 nm by controlling the reaction temperature. The following reactions can be summarized for this entire

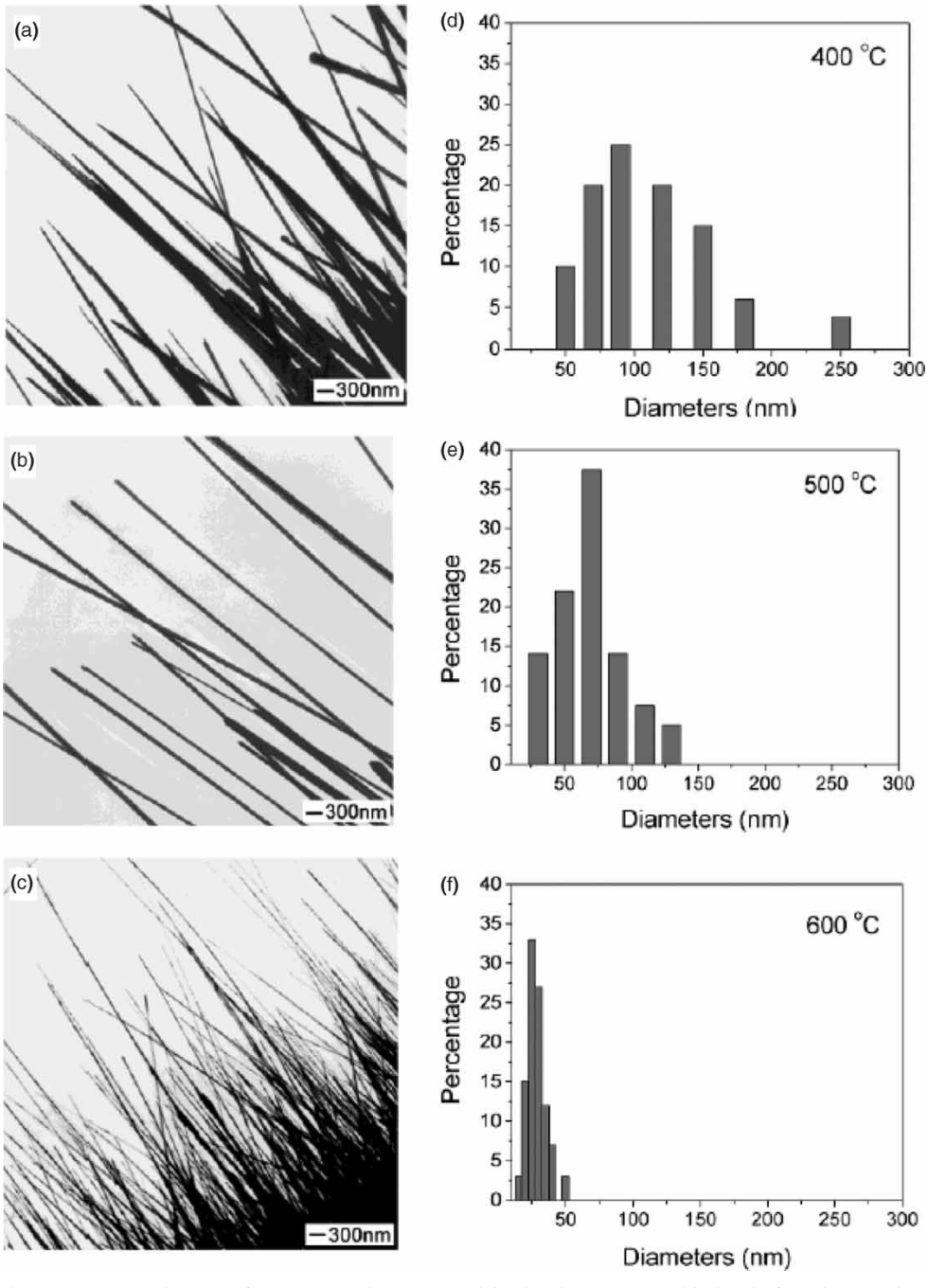

Figure 27. TEM images of CuO nanowires prepared by heating copper grids in air for 4 h at various temperatures: (a) 400°C, (b) 500°C, and (c) 600°C. The corresponding size distributions of these nanowires are shown in graphs D to F. These results suggest that the diameter of the CuO nanowires could be varied in the range of 30–100 nm by controlling the reaction temperature [50].

synthesis, with the second one being as the rate-determining step for the formation of CuO vapour [51].

$$4Cu + O_2 \longrightarrow 2Cu_2O$$
$$2Cu_2O + O_2 \longrightarrow 4CuO$$

The slow rate for the formation of CuO ensures a relatively low vapour pressure is required for this material in the reaction chamber, which helps for a continuous growth mode and uniform diameter for the CuO nanowires.

Similarly, Yu *et al.* [52] reported preparation of CuO nanorods of diameter 20–150 nm and length of several micrometers by annealing the copper plate at 400°C for 24 h in air. However, Huang *et al.* [53] prepared large scale of CuO nanowires by thermal evaporation of copper foil at various temperatures (300–800°C) under an oxygen flow rate of about 50 ml/min. Also, they determined that the diameter and length of nanowires vary with the evaporation temperature and time. For example, SEM images (figure 28) show the morphologies of the samples prepared at various temperatures and they also proposed growth mechanism similar to Xia *et al.* [50].

Though preparation of CuO nanoparticles by different approaches are mentioned above, Yang *et al.* [54] obtained CuO nanoribbon arrays on copper converted from $Cu(OH)_2$ nanoribbon arrays prepared by solution-solid reactions. That is, copper foil was washed with a 4 M HCl aqueous solution and subsequently with deionized water repeatedly to remove surface impurities. The washed copper foil was then immersed into a dilute solution of ammonia (3.3×10^{-2} M, pH $\approx$ 10) for certain periods of time (12–96 h) and then taken out of the solution, washed with deionized water. The blue film covered uniformly on the Cu substrate was found to be $Cu(OH)_2$ nanoribbon arrays, which was confirmed by SEM analysis (figure 29). To get CuO nanoribbons, the above prepared $Cu(OH)_2$ nanoribbon sample was loaded into a quartz boat and heated in a furnace under constant flow of N_2 ($\sim$25 sccm) at 120°C for 3 h to get dehydration and then heated at 180°C for 2 h to promote crystallization. Adopting this procedure, CuO nanoribbons (figure 30) were obtained with an average width of $\sim$50–60 nm and several nanometers long by varying the reaction time and temperature interval. The reactions that account for the formation of $Cu(OH)_2$ and CuO nanoribbons probably proceed as follows:

$$Cu + O_2 + NH_3 \longrightarrow Cu[NH_3]_n^{2+}$$
$$Cu[NH_3]_n^{2+} + OH^- \longrightarrow Cu(OH)_2$$
$$Cu(OH)_2 \xrightarrow{\Delta} CuO$$

In addition, they also prepared CuO nanorod arrays [55] at ambient temperature conditions (without heating) as follows. Washed copper foil was immersed into 400 ml of water containing various amounts of ammonia (13 M) and NaOH (1 M) solutions at

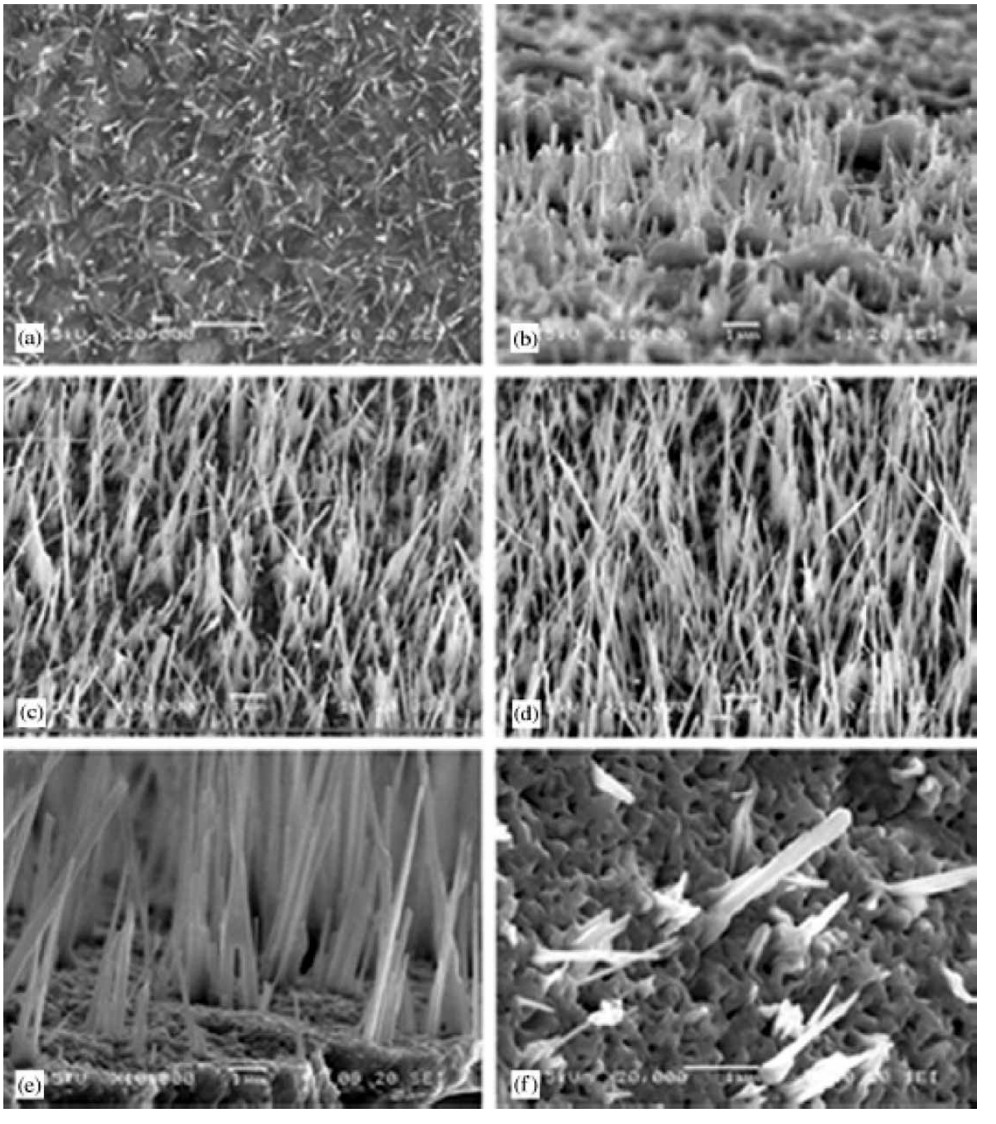

Figure 28. SEM images of CuO nanowires prepared at various temperatures: (a) 300°C, (b) 400°C, (c) 500°C, (d) 600°C, (e) 750°C and (f) 800°C [53].

room temperature for certain period of time. After a given reaction time, the sample was taken out of the solution, washed with deionized water, and dried in air. A black film covered uniformly on the Cu substrate. This was found to be CuO nanorod, which was confirmed by SEM analysis (figure 31). The reactions are almost same as above but the third reaction occurs at room temperature for this system. The main reason for such effect is that the solution is more basic here, so that $Cu(OH)_2$ is unstable and thus immediately decomposed to CuO. By adopting this simple wet chemical method at

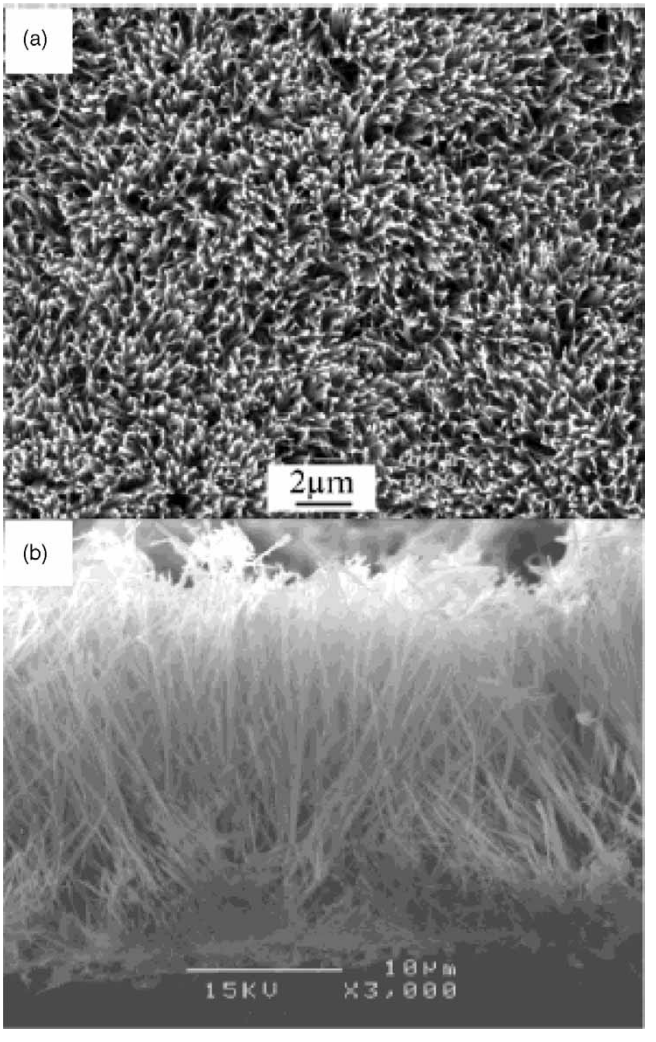

Figure 29. SEM images of a $Cu(OH)_2$ nanoribbon array. (a) Top view. (b) Side view [54].

room temperature vertically aligned CuO nanorod arrays on copper electrodes with diameters of ~5 nm and lengths of hundreds of nanometers were obtained. Also, they used as-prepared CuO nanorod arrays as cathode for fabrication of dye-sensitized solar cells.

5. Conclusion

In summary, copper oxide nanoparticles of different crystalline structures and morphologies were synthesized successfully starting from the corresponding salts,

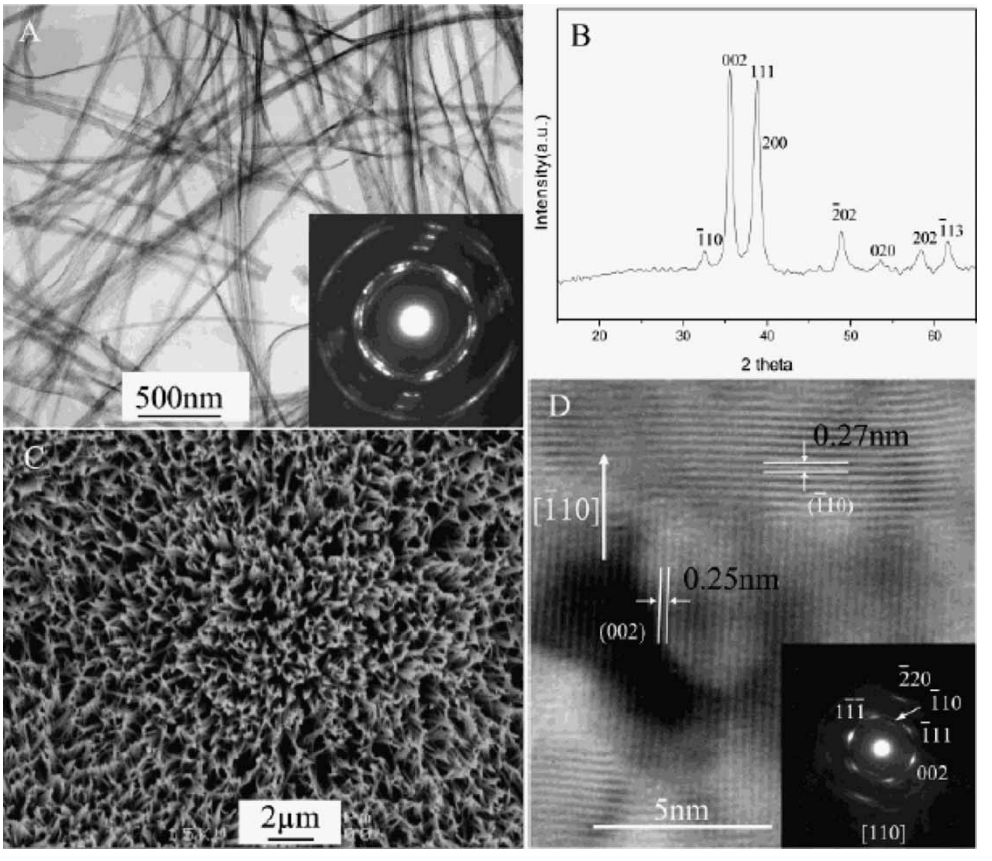

Figure 30. TEM image (a), XRD pattern (b), SEM image (c), and HRTEM image (d) of CuO nanoribbons converted from the $Cu(OH)_2$ nanoribbons by heat treatment. Inset of part A: SAED pattern of an ensemble of CuO nanoribbons. Inset of part D: SAED pattern of a single CuO nanoribbon [54].

acids and metal. Each method available here has its own significant advantages in preparing CuO nanoparticles of particular morphology and structure. But in order to identify which is the best method for large-scale production many factors (cost effective, preparation conditions, required facilities, etc) are to be taken into account. A great variety of procedures are mentioned in this paper, giving rise to the possibility of constituting a nanotoolbox for a ''bottom-up'' approach in nanoscience and nanotechnology. From the results, it is hoped that preparation of CuO nanoparticles will provide the impetus for solution-phase chemical synthesis to be considered as the most promising route in terms of cost, throughput, and the potential for large-scale production.

Overall, we are happy if the present survey gives researchers an opportunity to explore available methods to synthesize semiconductor CuO nanomaterials from different source materials. Thus, the given examples here illustrate the most impressive methods, which are available in the preparation of CuO nanomaterials in view of the

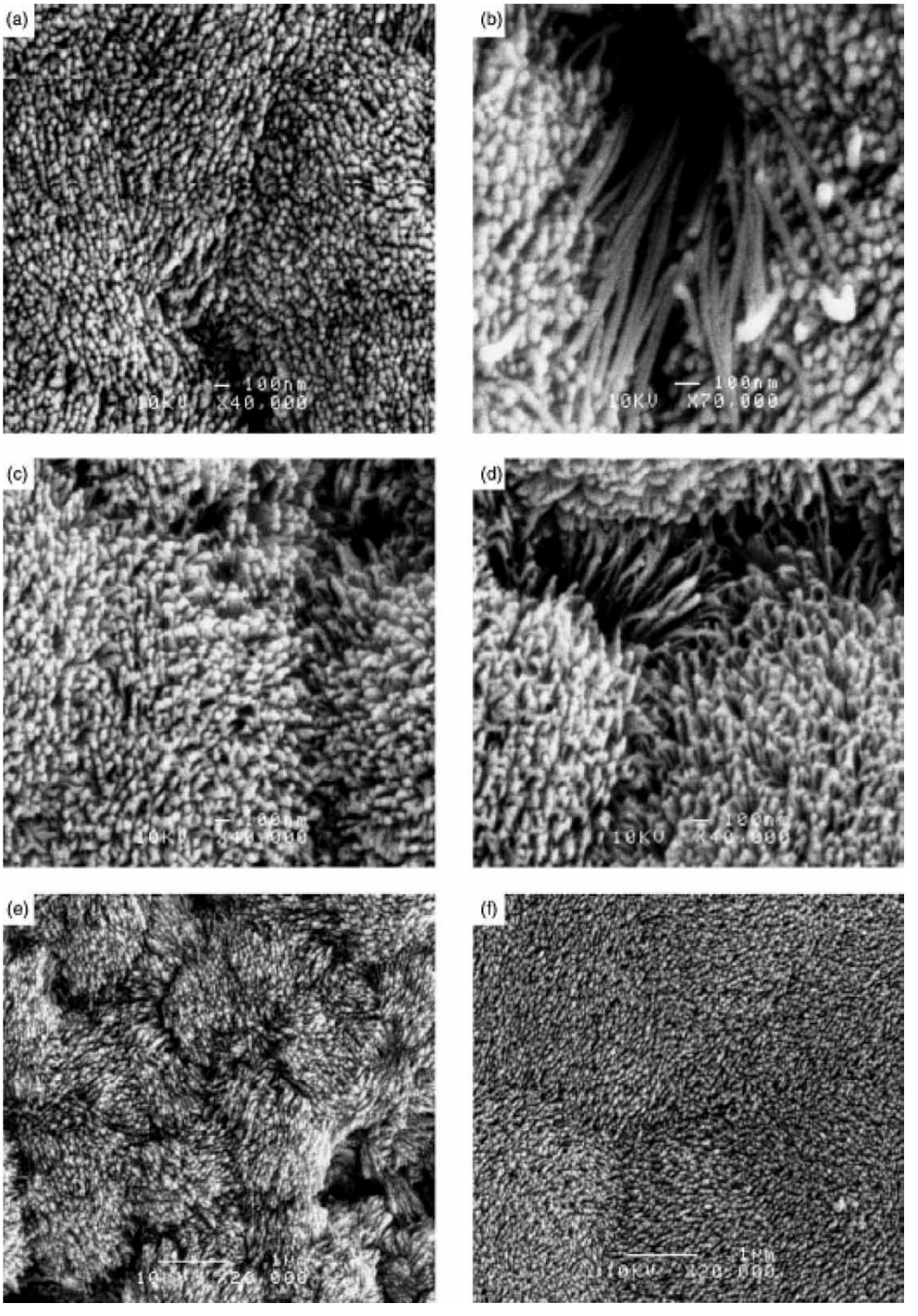

Figure 31. SEM images of p-CuO nanorods prepared at various pH and reaction time intervals: (a) pH 11 (96 h); (b) pH 11 (130 h); (c) pH 11.5 (96 h); (d) pH 11.5 (120 h); (e) pH 12 (96 h); (f) pH 12.3 (14 days) [55].

nano-science. The investigation of nano-science will remain a challenging task in the near future until it is regarded as a genuine field of science.

Acknowledgements

Author (SA) wishes to thank DST, New Delhi for the Fast Track Young Scientist award and The Director of the National Institute of Technology, Trichy, for providing funding from the TEQIP programme to create a new lab (Nanomaterials and Solar Energy Conversion).

References

[1] Z.L. Wang (Ed.). *Nanowires and Nanobelts*: *Materials, Properties and Devices*, Vol. 1–2, Kluwer Academic Publisher, Boston (2003)
[2] S. Iijima, T. Ichihashi. Single-shell carbon nanotubes of 1 nm diameter. *Nature*, **363**, 603 (1993).
[3] J.G. Wen, J.Y. Lao, D.Z. Wang, T.M. Kyaw, Y.L. Foo, Z.F. Ren. Self-assembly of semiconducting oxide nanowires, nanorods, and nanoribbons. *Chem. Phys. Lett*., **372**, 717 (2003).
[4] G.R. Patzke, F. Krumeich, R. Nesper. Oxidic nanotubes and nanorods – anisotropic modules for a future nanotechnology. *Angew. Chem. Int. Ed.*, **41**, 2446 (2002).
[5] F.R.N. Nabarro, P.J. Jackson, Growth of crystal whiskers, in *Growth and Perfection of Crystal Growth*, R.H. Doremus, B.W. Roberts and D. Turnbull (Eds), pp. 13–120, Wiley, New York (1958).
[6] T.S. Ahmadi, Z.L. Wang, T.C. Green, A. Henglein, M.A. El-Sayed. Shape-controlled synthesis of colloidal platinum nanoparticles. *Science*, **272**, 1924 (1996).
[7] V. Albe, C. Jouanin, D. Bertho. Influence of II–VI nanocrystal shapes on optical properties. *J. Cryst. Growth*, **185**, 388 (1998).
[8] A.M. Morales, C.M. Lieber. A laser ablation method for the synthesis of crystalline semiconductor nanowires. *Science*, **279**, 208 (1998).
[9] C.R. Martin. Nanomaterials – a membrane-based synthetic approach. *Science*, **266**, 1961 (1994).
[10] Y.D. Wang, C.L. Ma, X.D. Sun, H.D. Li. Preparation of nanocrystalline metal oxide powders with the surfactant-mediated method. *Inorg. Chem. Commun*., **5**, 751 (2002).
[11] W.S. Shi, Y.F. Zheng, N. Wang, C.S. Lee, S.T. Lee. A general synthetic route to III–V compound semiconductor nanowires. *Adv. Mater*., **13**, 591 (2001).
[12] Z.W. Pan, Z.R. Dai, Z.L. Wang. Nanobelts of semiconducting oxides. *Science*, **291**, 1947 (2001).
[13] S.W. Liu, J. Yue, A. Gedanken. Synthesis of long silver nanowires from AgBr nanocrystals. *Adv. Mater*., **13**, 656 (2001).
[14] Y.D. Li, H.W. Liao, Y. Ding, Y.T. Qian, Y. Li, G.E. Zhou. Nonaqueous synthesis of CdS nanorod semiconductor. *Chem. Mater*., **10**, 2301 (1998).
[15] W.Z. Wang, Y. Geng, P. Yan, F.Y. Liu, Y. Xie, Y.T. Qian. Synthesis and characterization of MSe (M = Zn, Cd) nanorods by a new solvothermal method. *Inorg. Chem. Commun*., **2**, 83 (1999).
[16] P. Yan, Y. Xie, Y.T. Qian, X.M. Liu. A cluster growth route to quantum-confined CdS nanowires. *Chem. Commun*., 1293 (1999).
[17] Z.X. Deng, C. Wang, X.M. Sun, Y.D. Li. Structure-directing coordination template effect of ethylenediamine in formations of ZnS and ZnSe nanocrystallites via solvothermal route. *Inorg. Chem*., **41**, 869 (2002).
[18] L. Manna, E.C. Scher, A.P. Alivisators. Synthesis of soluble and processable rod-, arrow-, teardrop-, and tetrapod-shaped CdSe nanocrystals. *J. Am. Chem. Soc*., **122**, 12700 (2000).
[19] Y. Qing, K.B. Tang, Ch.R. Wang, Y.T. Qian, Sh.Y. Zhang. PVA-assisted synthesis and characterization of CdSe and CdTe nanowires. *J. Phys. Chem. B*, **106**, 9227 (2002).
[20] C.C. Chen, C.Y. Chao, Z.H. Lang. Simple solution-phase synthesis of soluble CdS and CdSe nanorods. *Chem. Mater*., **12**, 1516 (2000).
[21] K.L. Hardee, A.J. Bard. Semiconductor electrodes X photoelectrochemical behavior of several polycrystalline metal oxide electrodes in aqueous solutions. *J. Electrochem. Soc*., **124**, 215 (1977).
[22] M. Hara, T. Kondo, M. Komoda, S. Ikeda, K. Shinohara, A. Tanaka, J.N. Kondo, K. Domen. Cu_2O as a photocatalyst for overall water splitting under visible light irradiation. *Chem. Commun*., 357 (1998).

[23] S. Nakayama, A. Kimura, M. Shibata, S. Kuwabata, T. Osakai. Voltammetric characterization of oxide films formed on copper in air. *J. Electrochem. Soc*., **148**, B467 (2001).
[24] K. Nagase, Y. Zhang, Y. Kodama, J. Kakuta. Dynamic study of the oxidation state of copper in the course of carbon monoxide oxidation over powdered CuO and Cu_2O. *J. Catal*., **187**, 123 (1999).
[25] J.F. Xu, W. Ji, Z.X. Shen, S.H. Tang, X.R. Ye, D.Z. Jia, X.Q. Xin. Preparation and characterization of CuO nanocrystals. *J. Solid State Chem*., **147**, 516 (1999).
[26] J.F. Xu, W. Ji, Z.X. Shen, W.S. Li, S.H. Tang, X.R. Ye, D.Z. Jia, X.Q. Xin. Raman spectra of CuO nanocrystals. *J. Raman Spectrosc*., **30**, 413 (1999).
[27] W. Wang, Y. Zhan, X. Wang, Y. Liu, C. Zheng, G. Wang. Synthesis and characterization of CuO nanowhiskers by a novel one-step, solid-state reaction in the presence of a nonionic surfactant. *Mater. Res. Bull*., **37**, 1093 (2002).
[28] J.H. Sun, Y.J. Gong, W.H. Fan, D. Wu, Y.H. Sun. *Chem. J. Chin. Univ*., **21**, 95 (2000).
[29] W. Wang, Z. Liu, Y. Liu, C. Xu, C. Zheng, G. Wang. A simple wet-chemical synthesis and characterization of CuO nanorods. *Appl. Phys. A*, **76**, 417 (2003).
[30] Joint Committee on Powder Diffraction Standards: diffraction Data File, No. 5–661, JCPDS International Center for Diffraction Data, Pennsylvania (1991)
[31] X.P. Gao, J.L. Bao, G.L. Pan, H.Y. Zhu, P.X. Huang, F. Wu, D.Y. Song. Preparation and electrochemical performance of polycrystalline and single crystalline CuO nanorods as anode materials for Li ion battery. *J. Phys. Chem. B*., **108**, 5547 (2004).
[32] A. Punnoose, H. Magnone, M.S. Seehra, J. Bonevich. Bulk to nanoscale magnetism and exchange bias in CuO nanoparticles. *Phy. Rev. B*, **64**, 174420 (2001).
[33] M.M. Ibrahim, J. Zhao, M.S. Seehra. Determination of the particle size distribution in Fe_2O_3-based catalyst using magnetometry and X-ray diffraction. *J. Mater. Res*., **7**, 1856 (1992).
[34] A. Viano, S.R. Mishra, R. Lloyd, J. Losby, T. Gheyi. Thermal effects on ESR signal evolution in nano and bulk CuO powder. *J. Non-crystal. Solids*, **325**, 16 (2003).
[35] C.L. Zhu, C.N. Chen, L.Y. Hao, Y. Hu, Z.Y. Chen. Template-free synthesis of $Cu_2Cl(OH)_3$ nanoribbons and use as sacrificial template for CuO nanoribbon. *J. Crys. Growth*, **263**, 473 (2004).
[36] C.L. Zhu, C.N. Chen, L.Y. Hao, Y. Hu, Z.Y. Chen. In-situ preparation of 1D CuO nanostructures using $Cu_2(OH)_2CO_3$ nanoribbons as precursor for sacrifice-template via heat-treatment. *Solid State Commun*., **130**, 681 (2004).
[37] X. Song, S. Sun, W. Zhang, H. Yu, W. Fan. Synthesis of $Cu(OH)_2$ nanowires at aqueous-organic interfaces. *J. Phys. Chem. B*, **108**, 5200 (2004).
[38] C. Lu, L. Qi, J. Yang, D. Zhang, N. Wu, J. Ma. Simple template-free solution route for the controlled synthesis of $Cu(OH)_2$ and CuO nanostructures. *J. Phys. Chem. B*, **108**, 17825 (2004).
[39] Y. Chang, H.C. Zeng. Controlled synthesis and self-assembly of single-crystalline CuO nanorods and nanoribbons. *Crys. Growth Des*., **4**, 397 (2004).
[40] B. Liu, H.C. Zeng. Formation of ''Dandelions''. *J. Am. Chem. Soc*., **126**, 8124 (2004).
[41] R. Yang, L. Gao. Novel way to synthesize CuO nanocrystals with various morphologies. *Chem. Lett*., **33**, 1194 (2004).
[42] E.S. Baker, J. Jonas. Transport and relaxation properties of dimethyl sulfoxide-water mixtures at high pressure. *J. Phys. Chem*., **89**, 1730, (1985), and the references cited therein.
[43] J. Nemeth, G. Rodriguez-Gattorno, D. Diaz, A.R. Vazquez-Olmos, I. Dekany. Synthesis of ZnO nanoparticles on a clay mineral surface in dimethyl sulfoxide medium. *Langmuir*, **20**, 2855 (2004).
[44] C.K. Xu, Y.K. Liu, G. Xu, G. Wang. Preparation and characterization of CuO nanorods by thermal decomposition of CuC_2O_4 precursor. *Mater. Res. Bull*., **37**, 2365 (2002).
[45] Z.S. Hong, Y. Cao, J.F. Deng. A convenient alcohothermal approach for low temperature synthesis of CuO nanoparticles. *Mater. Lett*., **52**, 34 (2002).
[46] H. Wang, J.Z. Xu, J.J. Zhu, H.Y. Chen. Preparation of CuO nanoparticles by microwave irradiation. *J. Crys. Growth*, **244**, 88 (2002).
[47] M. Iwasaki, S. Ito. New route to prepare ultrafine ZnO particles and its reaction mechanism. *J. Mater. Sci. Lett*., **16**, 1503 (1997).
[48] K. Borgohain, J.B. Singh, M.V. Rama Rao, T. Shripathi, S. Mahamumi. Quantum size effects in CuO nanoparticles. *Phy. Rev. B*., **61**, 11093 (2000).
[49] C.H. Lo, T.T. Tsung, L.C. Chen, C.H. Su, H.M. Lin. Fabrication of copper oxide nanofluid using submerged arc nanoparticle synthesis system (SANSS). *J. Nanopar. Res*., **7**, 313 (2005).
[50] X. Jiang, T. Herricks, Y. Xia. CuO nanowires can be synthesized by heating copper substrate in air. *Nano Lett*., **2**, 1333 (2002).
[51] G.A. Adegboyega. Preparation and characterization of thermally oxidized copper substrates for photothermal and photovoltaic energy conversion. *Niger, J. Renew. Energy*, **1**, 21 (1990).
[52] T. Yu, X. Zhao, Z.X. Shen, Y.H. Wu, W.H. Su. Investigation of individual CuO nanorods by polarized micro-Raman scattering. *J. Crys. Growth*, **268**, 590 (2004).

[53] L.S. Huang, S.G. Yang, T. Li, B.X. Gu, Y.W. Du, Y.N. Lu, S.Z. Shi. Preparation of large-scale cupric oxide nanowires by thermal evaporation method. *J. Crys. Growth*, **260**, 130 (2004).
[54] X.G. Wen, W.X. Zhang, S.H. Yang. Synthesis of $Cu(OH)_2$ and CuO nanoribbon arrays on a copper substrate. *Langmuir*, **19**, 5898 (2003).
[55] S. Anandan, X.G. Wen, S.H. Yang. Room temperature growth of CuO nanorod arrays on copper and their application as a cathode in dye-sensitized solar cells. *Mater. Chem. Phys.*, **93**, 35 (2005).